

Equivalent Circuit Analysis of the RHIC Injection Kicker

H. Hahn

April 1997

Collider Accelerator Department
Brookhaven National Laboratory

U.S. Department of Energy

USDOE Office of Science (SC)

Notice: This technical note has been authored by employees of Brookhaven Science Associates, LLC under Contract No. DE-AC02-76CH00016 with the U.S. Department of Energy. The publisher by accepting the technical note for publication acknowledges that the United States Government retains a non-exclusive, paid-up, irrevocable, world-wide license to publish or reproduce the published form of this technical note, or allow others to do so, for United States Government purposes.

DISCLAIMER

This report was prepared as an account of work sponsored by an agency of the United States Government. Neither the United States Government nor any agency thereof, nor any of their employees, nor any of their contractors, subcontractors, or their employees, makes any warranty, express or implied, or assumes any legal liability or responsibility for the accuracy, completeness, or any third party's use or the results of such use of any information, apparatus, product, or process disclosed, or represents that its use would not infringe privately owned rights. Reference herein to any specific commercial product, process, or service by trade name, trademark, manufacturer, or otherwise, does not necessarily constitute or imply its endorsement, recommendation, or favoring by the United States Government or any agency thereof or its contractors or subcontractors. The views and opinions of authors expressed herein do not necessarily state or reflect those of the United States Government or any agency thereof.

RHIC PROJECT

Brookhaven National Laboratory

Equivalent Circuit Analysis of the RHIC Injection Kicker

H. Hahn and A. Ratti

April 1997

EQUIVALENT CIRCUIT ANALYSIS OF THE RHIC INJECTION KICKER

H. Hahn and A. Ratti

INTRODUCTION

The RHIC injection kicker was conceived as a transmission line magnet in order to achieve the required rise time of <95 nsec. Using a CERN-type "plate-kicker" is the quasi-standard solution to achieve fast rise times.¹ However, following concepts contemplated at SLAC,^{2,3} a kicker configuration in which the lumped capacitors are replaced by high-permittivity ceramic blocks was adopted since it promised to be simpler, more compact, and more economical. The original design for the RHIC injection kicker was generated by Forsyth, et al,⁴ and a kicker R&D program was started in 1993. After implementing minor engineering changes to improve the high-voltage performance and to suppress coupling impedance resonances, four production kicker units, each with 1.12 m effective length, were fabricated in 1996 and successfully operated at ~ 32 kV and 1.6 kA in the "Sextant Test" to deflect the gold beam.

The kicker is configured from ferrite and dielectric blocks as a "C" type magnet with its geometry shown in Fig. 1. The deflecting properties of the kicker are dominated by the magnetic field and thus by the geometry and properties of the ferrite blocks. The nickel-zinc ferrite (CMD-5005 by Ceramic Magnetics) has a high permeability and resistivity for use at frequencies up to ~ 100 MHz. Although in principle continuous at the side, the ferrite must be subdivided to limit eddy current effects. The capacity required to achieve the transmission line behavior is predominantly provided by the dielectric ceramic blocks, a sintered mixture of magnesium and calcium titanate (MCT-100 or MCT-125 by Trans-Tech) with high dielectric constant. The four production kickers have dielectric blocks with $\epsilon = 100$, but subsequent magnets have been built with $\epsilon = 125$ to achieve the characteristic impedance of 25Ω . The contribution to the capacity from the ceramic beam tube is negligible, and for convenience sake, all kicker measurements were made without it.

The electrical properties of a transmission line kicker are in zeroth order established by its inductance, $\langle L \rangle$, and capacity, $\langle C \rangle$, per unit length. At sufficiently high permeability of the ferrite, the inductance is fully determined by the aperture requirements. The capacity must then be chosen to obtain the design characteristic impedance, in the case of the RHIC kicker 25Ω . In zeroth order, the characteristic impedance also determines the propagation velocity, $v/c \approx 0.066$ and the propagation time through the 1.12 m long kicker, $t \approx 56$ nsec. The rise time of the effective deflecting strength is obtained by folding the current rise time and the propagation time. The current rise time cannot be estimated from the model of an ideal transmission line, but

¹D. Fiander, Proc. 1971 Part. Acc. Conf., Chicago, IEEE Trans. NS-18, p.1022 (1971).

²F. Bulos and A. Odian, Report SLAC-PUB-3453, CN-279 (1984).

³R. Cassel, (private communication).

⁴E. B. Forsyth, G. C. Pappas, J. E. Tuozzolo, and W. (Arlene) Zhang, Proc. Particle Accelerator Conf., Dallas, TX p. 1921 (1996).

requires the information about the cell structure of the kicker. A convenient, and in practice the only way, to estimate the effective rise time is by means of equivalent circuit analysis.

The original kicker design by Forsyth was based on an equivalent circuit analysis of a low pass filter with lumped L and C elements. In a subsequent paper by Hahn and Forsyth,⁵ the kicker was treated as a transmission line with uniform, albeit anisotropic properties in order to establish a better correlation of geometrical with electrical parameters. In an attempt to estimate the current rise time from the low pass band width, the kicker was treated as a cascaded chain of transmission lines with different characteristic impedances and propagation velocities.⁶

Although useful, the simple equivalent circuits presented so far are limited and do not allow a reliable prediction of the kicker performance resulting from engineering changes or under varied operational conditions, such as the mismatched 20Ω termination used in the Sextant test. In this paper, an equivalent circuit for a generalized low-pass filter with lumped L , C , and R elements is presented, which was obtained from direct measurements of the kicker in the frequency range up to ~ 100 MHz. The P-Spice program was then used to simulate the kicker performance and the comparison with experimental data showed fully satisfactory agreement.

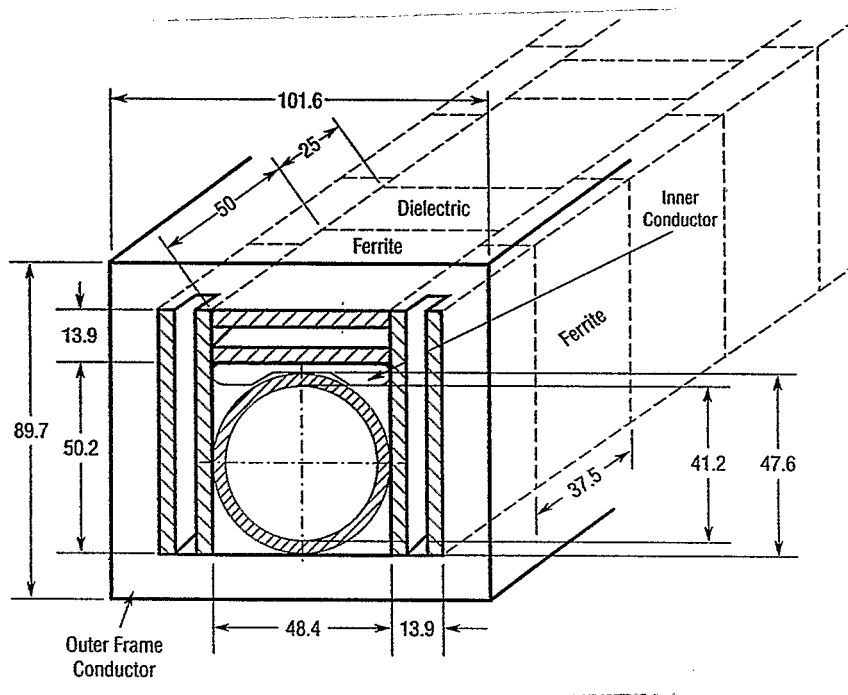


Fig. 1. RHIC Injection Kicker Configuration (dimensions in mm).
Only the end blocks are slotted

⁵H. Hahn and E. B. Forsyth, EPAC 94 London, vol. 3, p. 2550.

⁶H. Hahn, BNL Report AD/RHIC/RD-66 (1994).

THE EQUIVALENT CIRCUIT

The RHIC injection kicker is constructed as a low pass filter with 14 cells, each 7.5 cm long, with alternating ferrite and high-permittivity dielectric sections, thereby approximating a transmission line magnet. The cell structure permits an analysis of the electrical properties of the kicker using an equivalent circuit with lumped L , C , and R elements. Their values are obtained directly from input impedance measurements of the full-size kicker. Discussed here in detail is the production kicker #5, in which the MCT-125 dielectric blocks are used.

The inductance is obtained from the input impedance at 1 MHz with the output port shorted, as seen in Fig. 2. The total inductance was measured to be 1.59 μH , resulting in 106 nH for each of the 15 series inductors. The capacitance is obtained from the input impedance at 1 MHz with the output port open, as seen in Fig. 3. The total capacitance was 1.99 nF, resulting in ~ 140 pF for each of the 14 MCT-125 dielectric blocks. The MCT-100 block is represented by ~ 115 pF. The pronounced resonance at 64 MHz can be represented by a lossy series resonance. This resonance is associated with eddy currents in the ferrite side blocks, as established by a series of measurements with side blocks of different lengths (see Appendix). The circuit elements, and in particular the damping resistors, were adjusted to render the strength of the resonances in the open and shorted condition.

At frequencies below the $\lambda/4$ resonance at 4.757 MHz, the input impedance of the shorted kicker is given by $Z_{\text{in}} = Z_{\text{K}} \tan(f/f_{\pi/2})$. From the values at 9° and 18° follows the characteristic impedance of the kicker as $Z_{\text{K}} \approx 26 \Omega$. The measured input impedance of the kicker terminated with the nominal 25 Ω is shown in Fig. 4.

Using the equivalent circuit shown in Fig. 5, the P-Spice computed input impedances for the output port shorted, open, and terminated in the design 25 Ω are compared with the measured results in Figs. 2, 3 and 4 respectively. As seen, the agreement is quite satisfactory and establishes the confidence, that dependable predictions of the kicker performance can be made based on the equivalent circuit diagram. Of interest are for example the kicker response to a step function voltage, the operation of the kicker with a 20 Ω termination to reduce the voltage requirement, and the use of the MCT-100 dielectric blocks.

In a recent report, Claus⁷ studied the theoretical kicker properties using the cascaded transmission line model of ref. 6 and recommended geometrical changes, the merits of which must be evaluated.

His analysis predicts 14 mini-stop bands, the lowest appearing at 12.012 MHz, stemming from "the mismatch generated by the added half length inductive sections at the ends." In contrast to his predictions, the kicker measurements show no indication of such resonances even though at the lowest frequencies the losses are minimal as seen from the quarter and half wave

⁷ J.Claus, Report AD/RHIC-140 (BNL-63953, 1996)

length resonances in Fig 2 and 3. In fact, this result is in agreement with theory, since an examination of the expression for the wave propagation in a periodic structure with uniform cells proves that its characteristic impedance is fully determined by one cell, and remains unchanged by mismatched terminations. Also, P-Spice computations with and without the half-length end ferrite blocks gave essentially identical results and showed no stop bands. Stop bands would result only if a cell within the kicker has a different geometry. Construction errors can in principle cause stop bands but are in practice sufficiently small and smeared out by the losses.

Furthermore, Claus suggested to increase the number of ceramic strips from 14 to ~100 in order to achieve a frequency independent characteristic impedance. In the absence of losses, this would be correct, but given the properties of the ferrite used no gain can be expected from shorter dielectric blocks. Increasing the number of cells increases the length required by the epoxy-filled gaps, each 0.75 mm wide, amounting to a loss of ~20% in capacity. Finally, the cost of the blocks is significantly increased by the machining time over the weight-dependent cost of the material, and economical considerations as well as the satisfactory performance of the RHIC kickers strongly favor the present design.

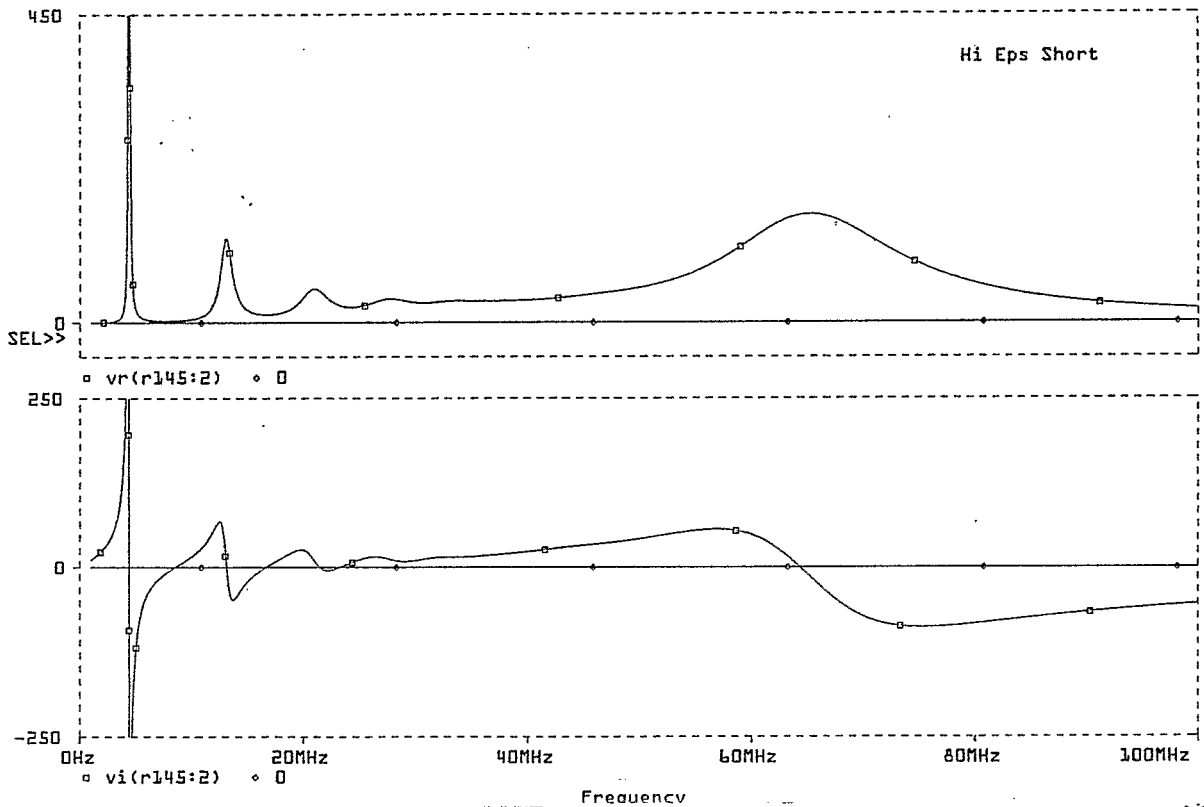
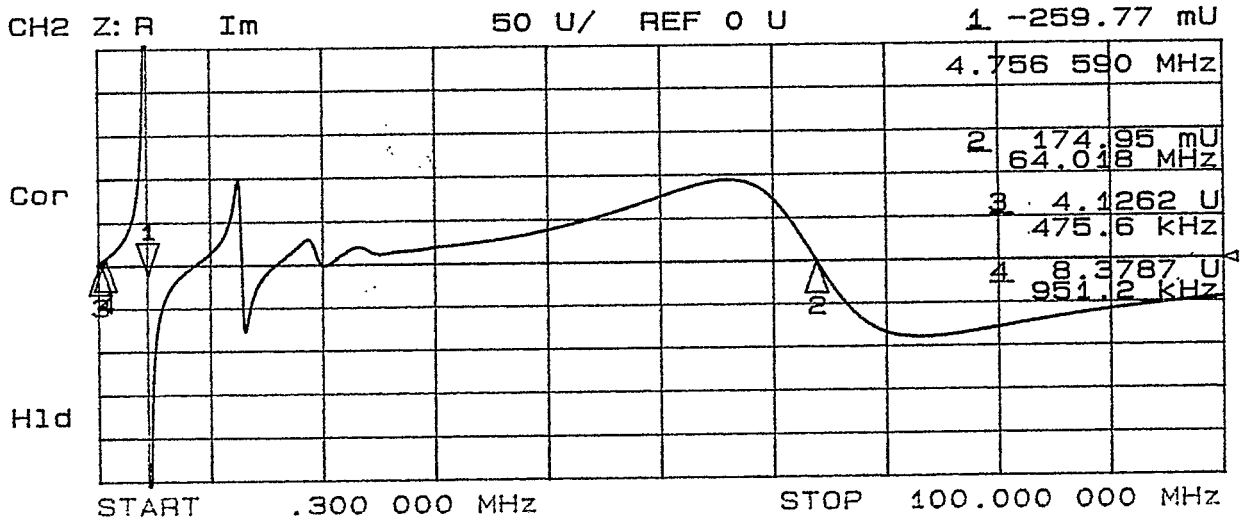
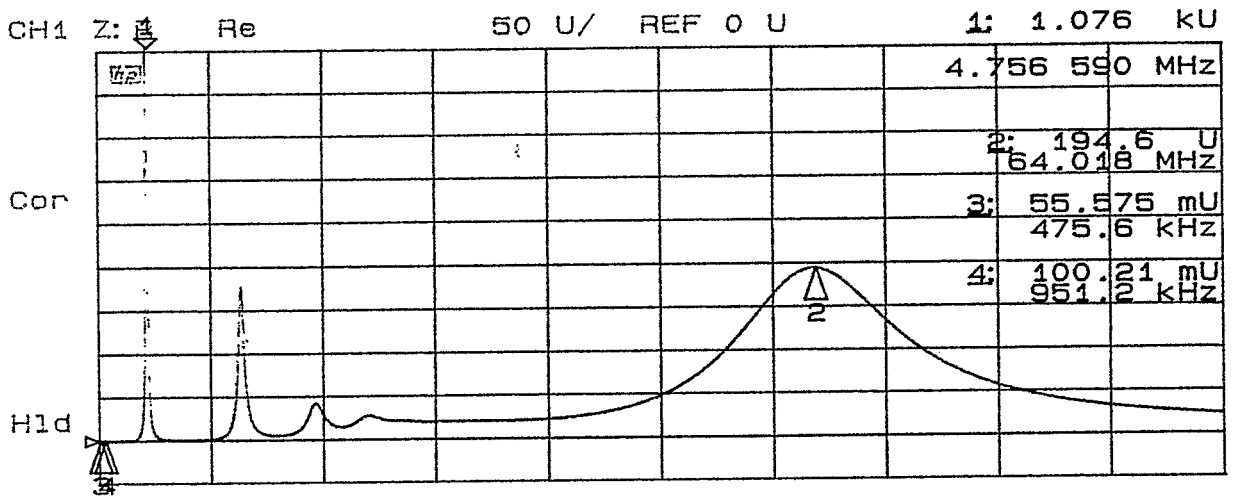


Fig. 2. Measured Input impedance of kicker with output port shorted and comparison with P-Spice computations.

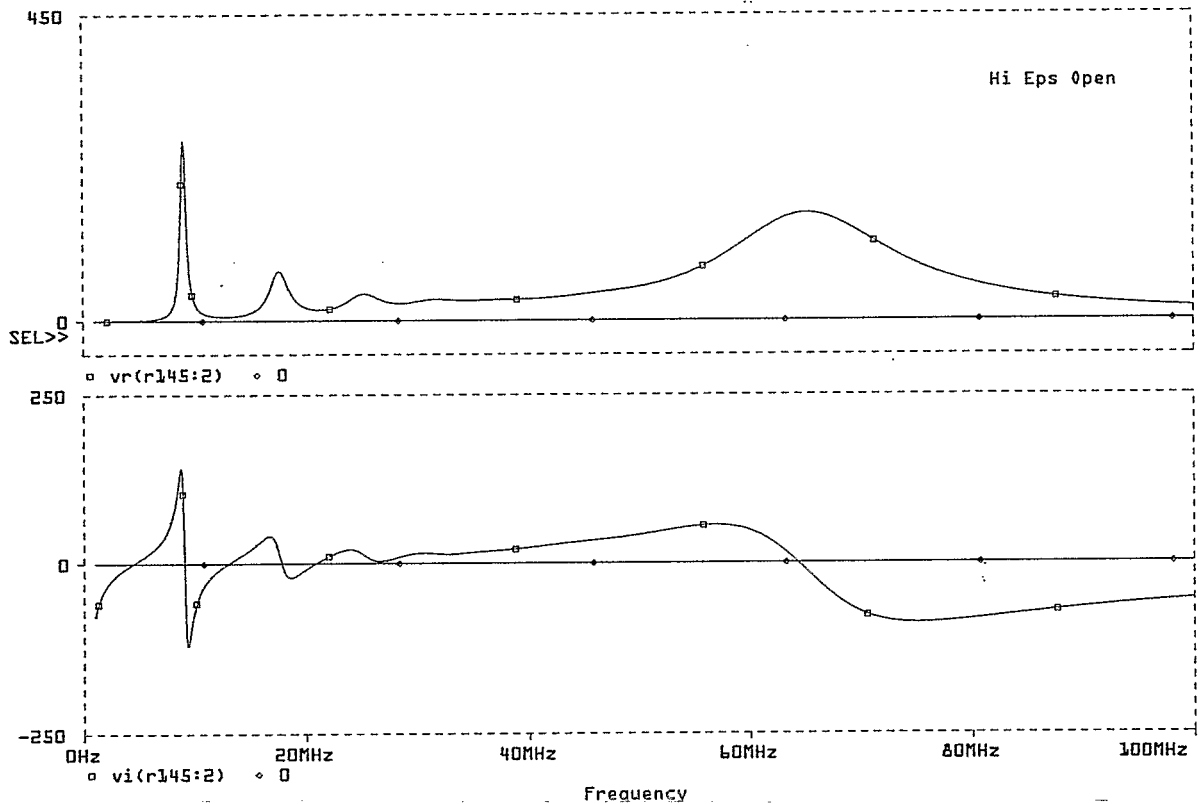
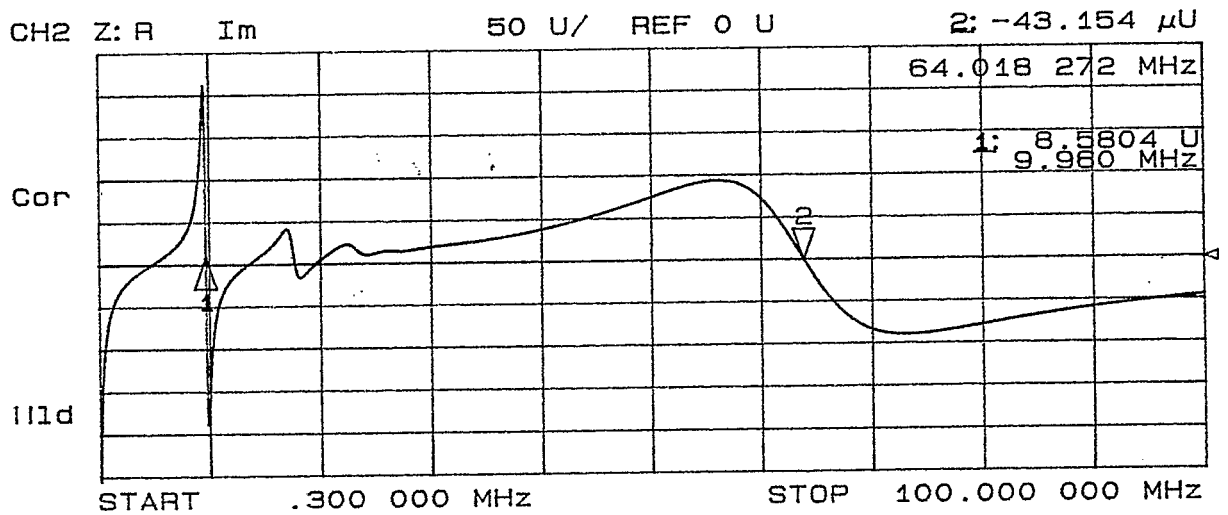
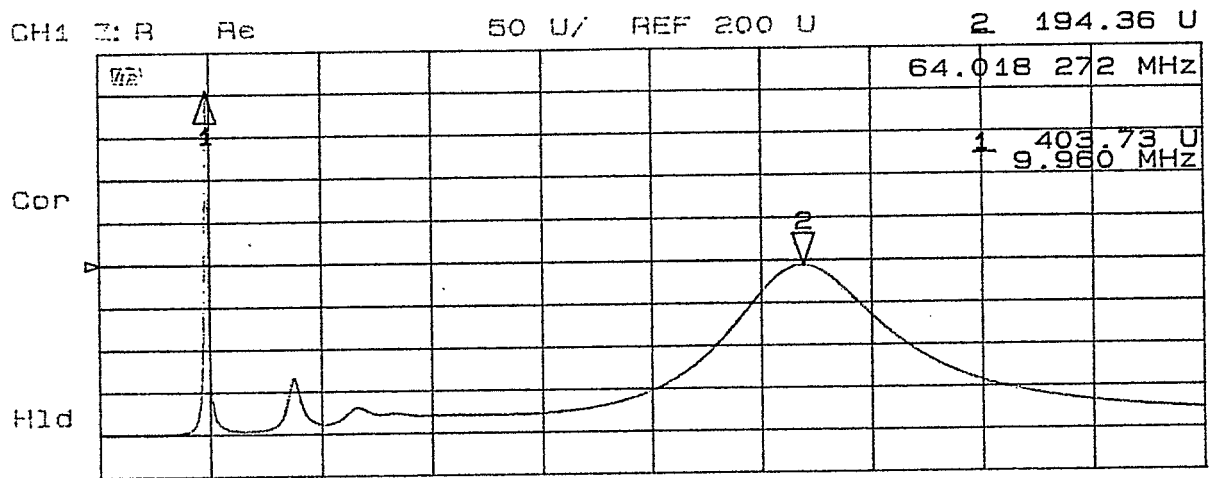


Fig. 3. Measured input impedance of kicker with output port open and comparison with P-Spice computations.

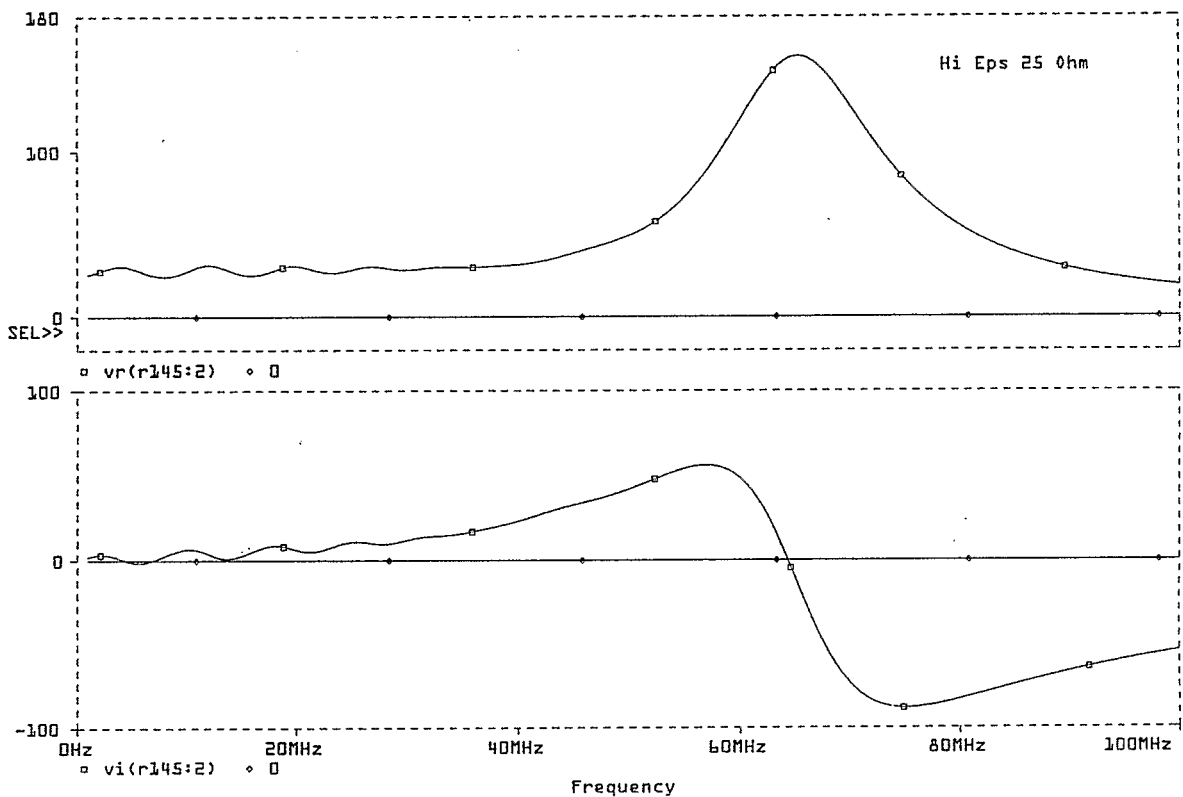
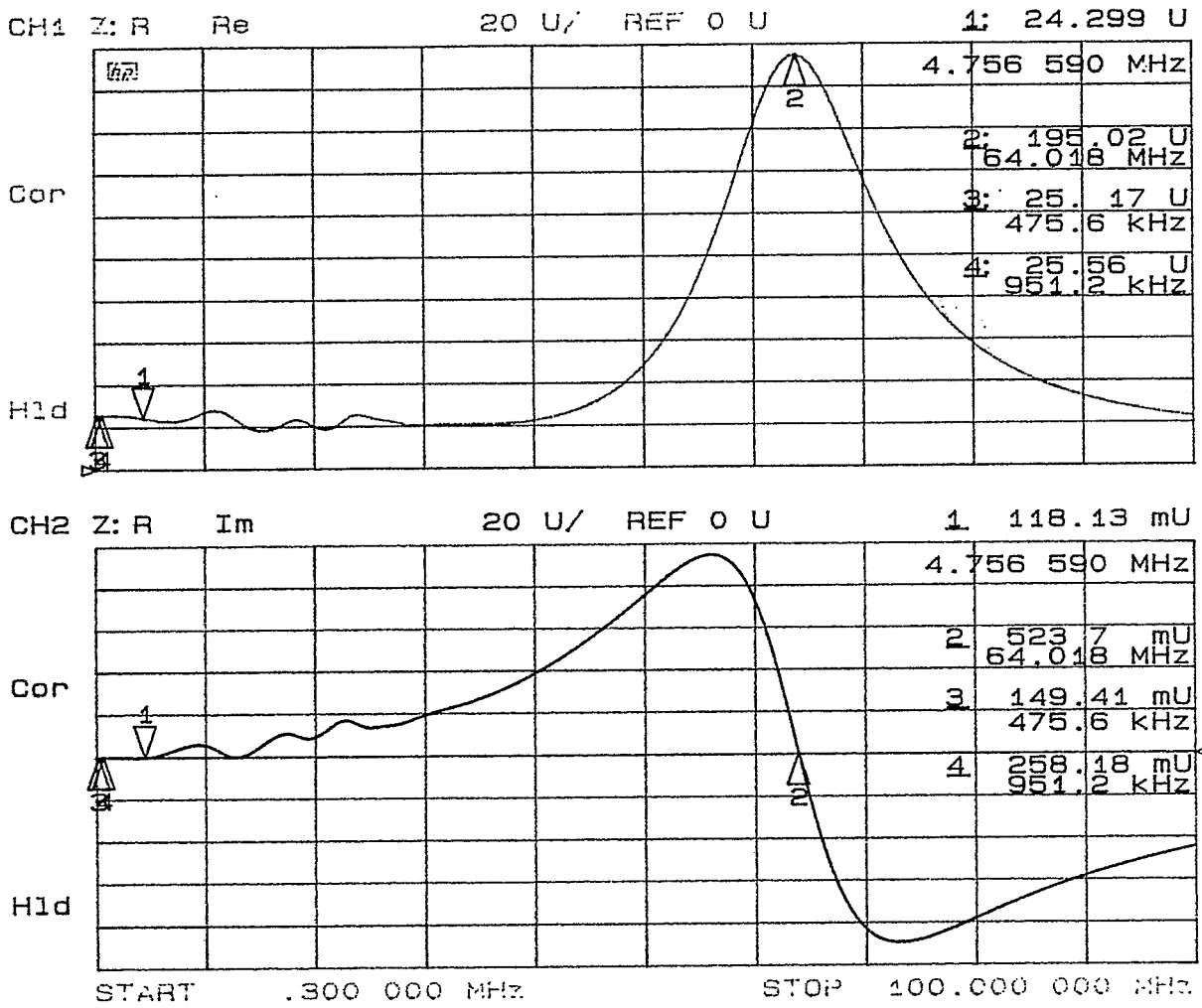


Fig. 4. Measured input impedance of kicker with matched output port termination and comparison with P-spice computations.

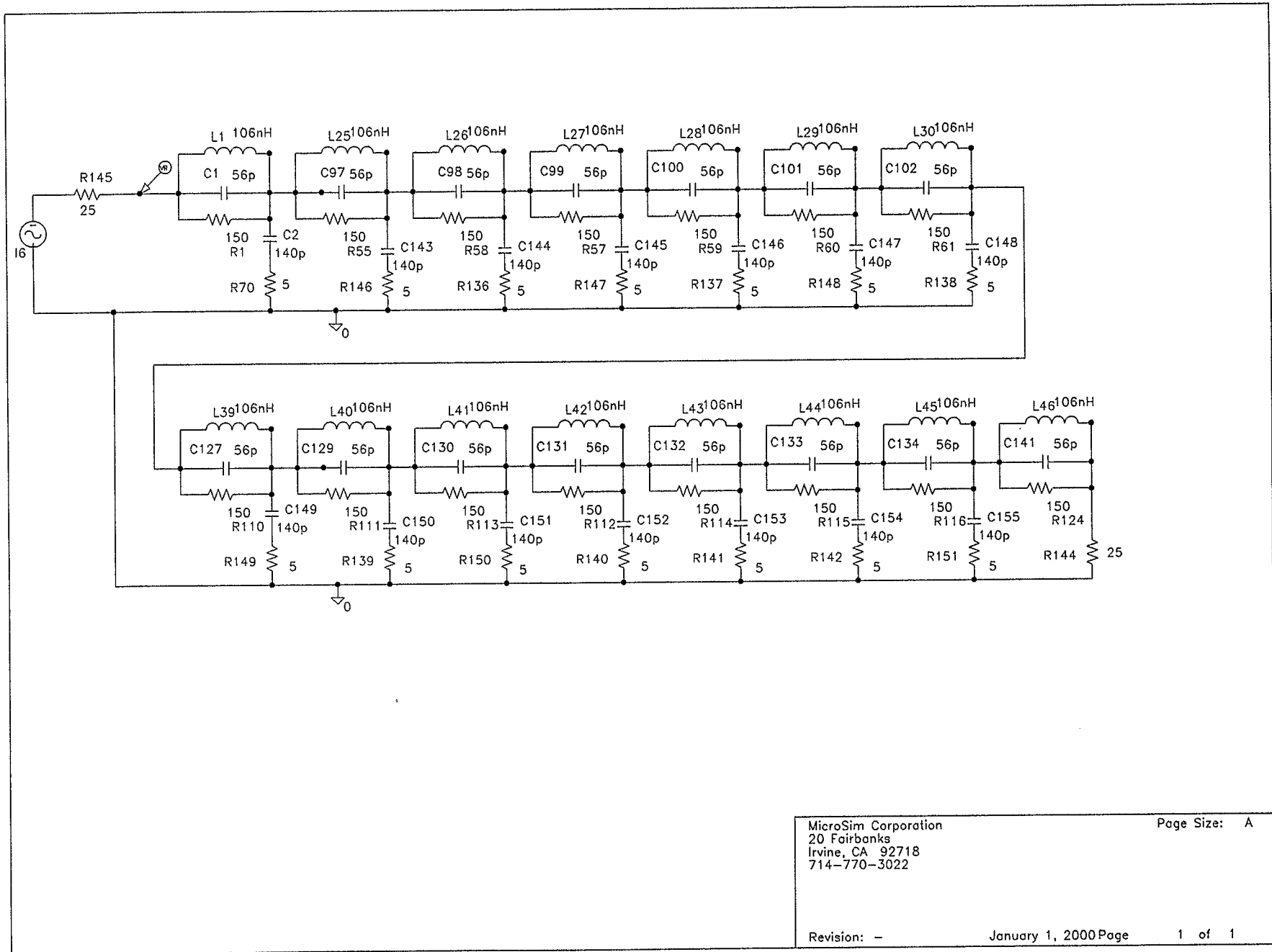


Fig. 5. Equivalent circuit of injection kicker.

COMPUTED AND MEASURED KICKER PERFORMANCE

Having established the equivalent circuit based on measurements in the frequency domain, it is now possible to predict the kicker performance in the time domain by means of P-Spice computations. Measurement of the performance of the kicker without beam is effectively limited to the current in the output load. The charging voltage on the Blumlein pulser can also be measured, but its value is not rigorously equal to the input voltage at the kicker.

The kicker load current in production unit #5 as measured with a current transformer is shown in Fig. 6 for a $25\ \Omega$ load for a ~ 40 kV pulser voltage, which satisfies the nominal design requirement of 1.6 kA. The measured current is in good agreement with the P-Spice computation. Also shown is the “effective kicker current,” which renders the rise time of the deflecting force and, neglecting the 3 nsec ion transit time, is obtained by averaging the instantaneous current in the 15 series inductors. The computed rise time of the effective current is ≤ 100 nsec in full agreement with the Sextant Test beam measurements⁸

In the Sextant Test, the kicker magnets were terminated with $20\ \Omega$ instead of the nominal $25\ \Omega$ resistors in order to gain safety margin against voltage breakdown. The measured load current for the two cases is shown in Fig. 7. The mismatch causes an “after-pulse,” about 850 nsec after the peak of the deflection, due to a reflected signal returning to the pulser and there being reflected again. The after-pulse, by serendipity, falls between the 4th and 5th beam pulse after the injected bunch, if the design 60-bunch injection is attempted. In any case, the after-pulse falls within the $\sim 1\ \mu\text{sec}$ beam dump gap. Also shown in Fig. 7 is the P-Spice computed effective current in the two cases (the dashed lines are from Fig. 6). One finds that in order to achieve the same peak deflection, or 1.6 kA effective, in the case of a mismatched $20\ \Omega$ load, the pulser voltage is reduced from 40 kV to only ~ 36.6 kV, even though the voltage on the load is lowered to 32.6 kV. A mismatched termination makes the effective current pulse less flat, which is, however, in the single-bunch transfer mode at RHIC of no consequence. In retrospect, one must conclude that mismatched operation is possible, but of marginal advantage.

The pulse propagation time in the 1.12 m long kicker was directly measured by means of uncalibrated capacitive probes at the input and output ends. The two signals are shown in Fig. 8; by using a single trigger, the propagation time was directly measured to be ~ 50 nsec, in excellent agreement with the theoretical prediction based on a propagation velocity of $c/v = 15$. The measured value is also in agreement with the computed P-Spice predictions as seen in Fig. 8.

⁸W. Fischer, H. Hahn, W. MacKay, D. Trbojevic, Proc. 1997 Particle . Acc. Conf., Vancouver, BC (to be published).

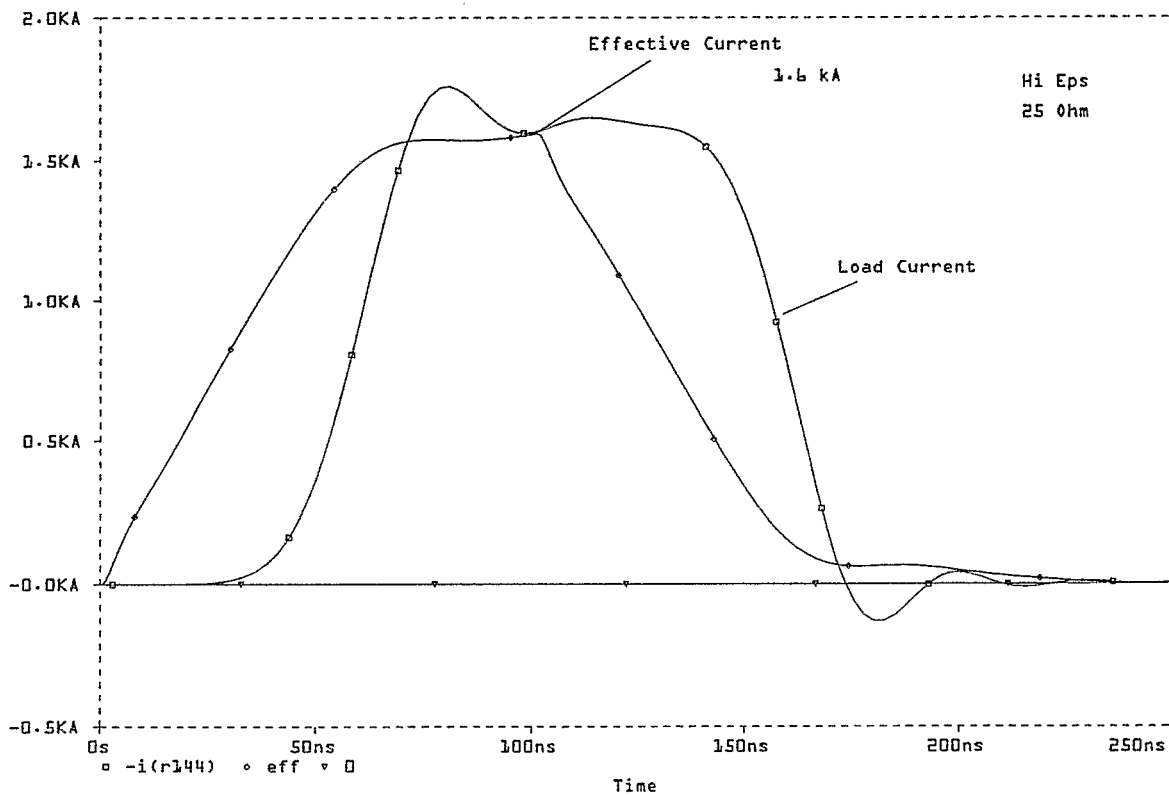
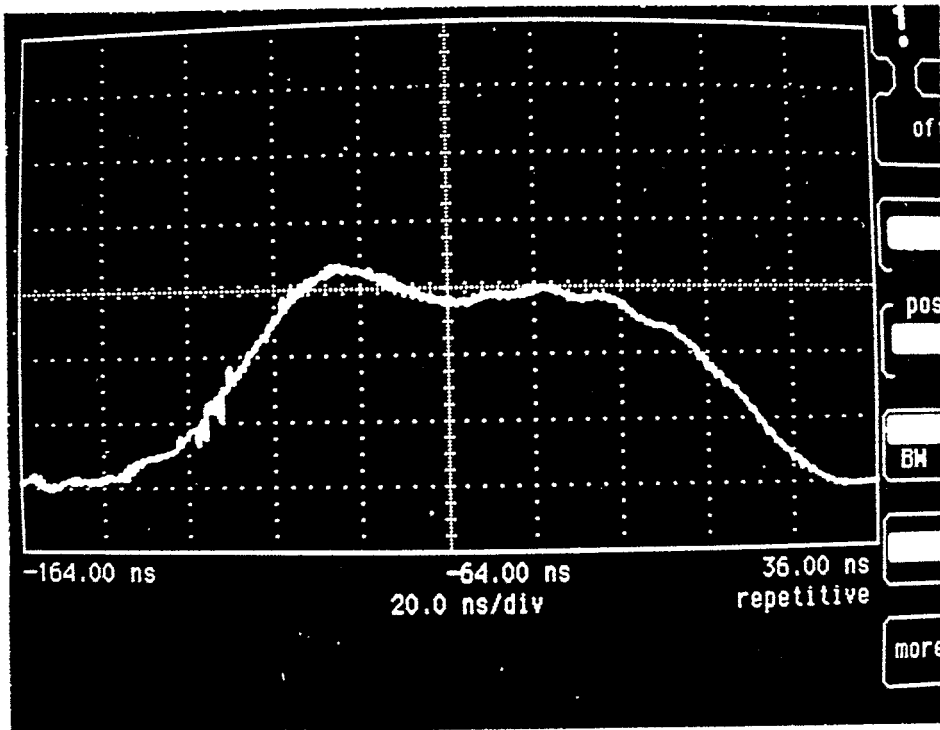


Fig. 6. Measured load current at 500 A/division and comparison with P-spice computed curve. The computed “effective” current represents the average of currents in the 15 series inductors and is an estimate of the time-dependent kicker deflecting strength.

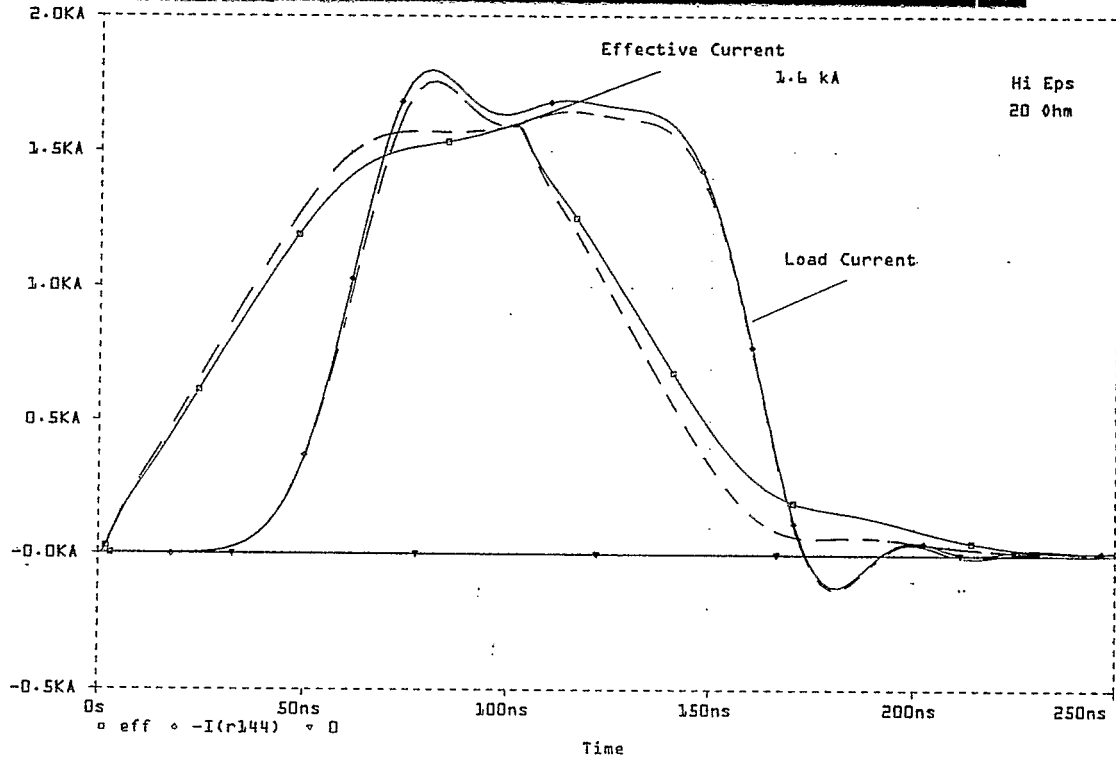
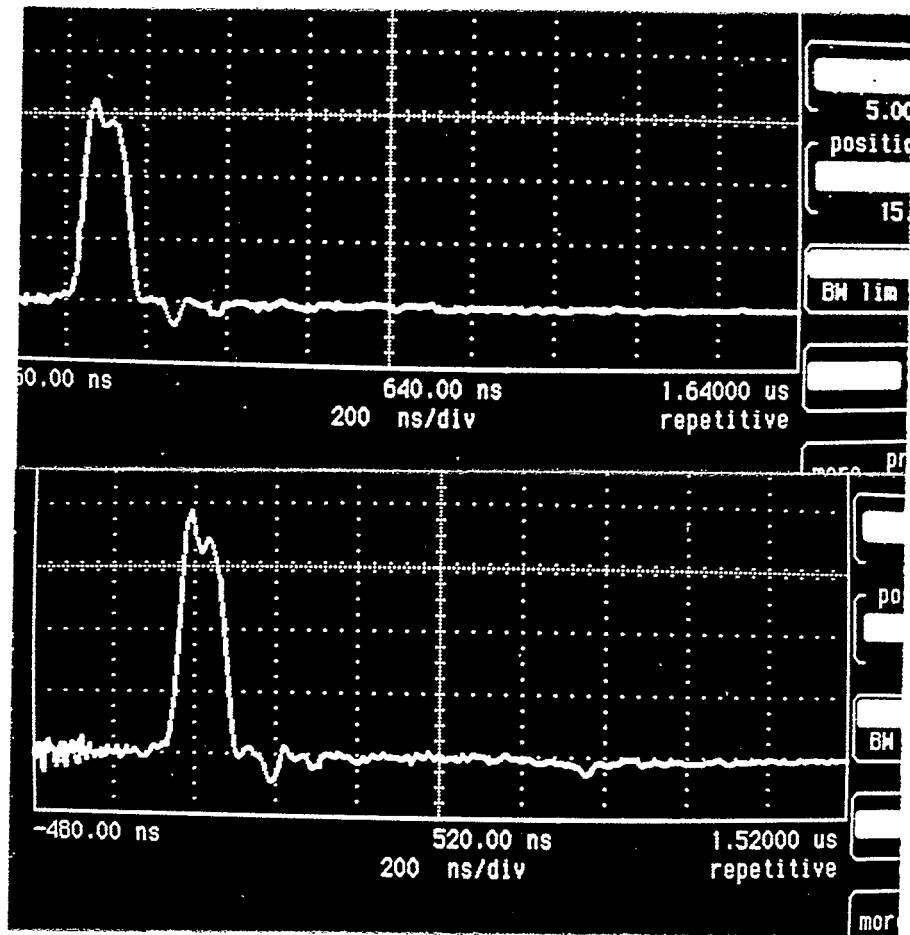


Fig. 7. Comparison of the measured load current in the case of a matched, 25Ω , and mismatched, 20Ω , load. Note the small after-pulse, ~ 850 nsec after the main pulse, in the mismatched case. Also shown are the P-Spice computed load currents for the matched (dashed line) and mismatched (solid line) terminations.

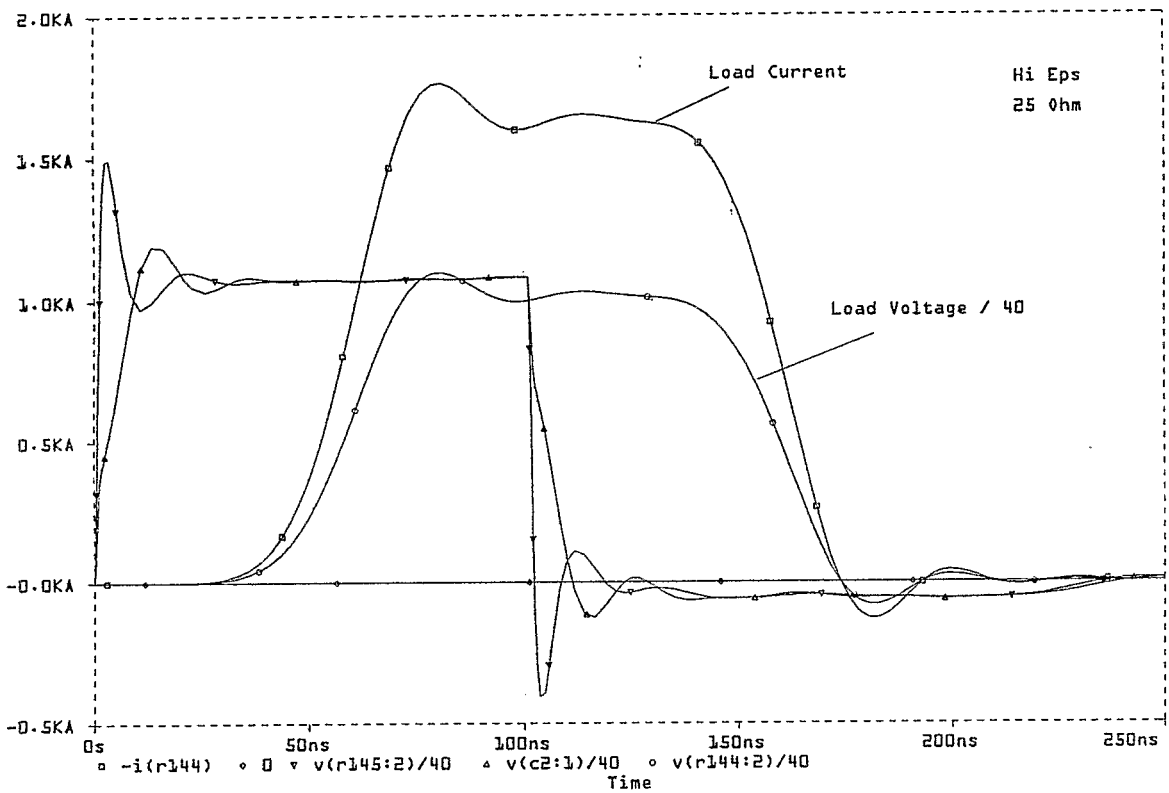
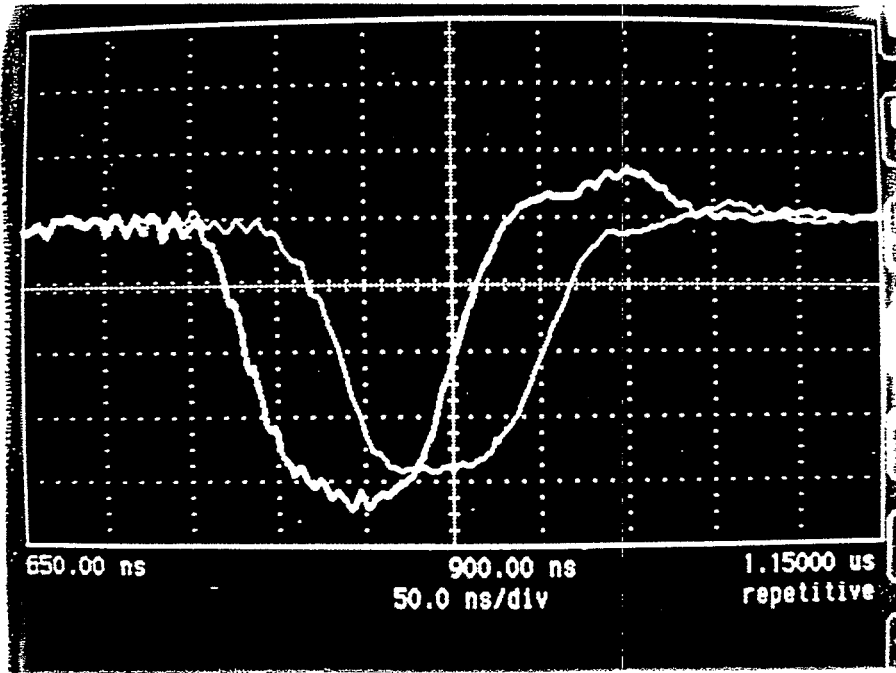
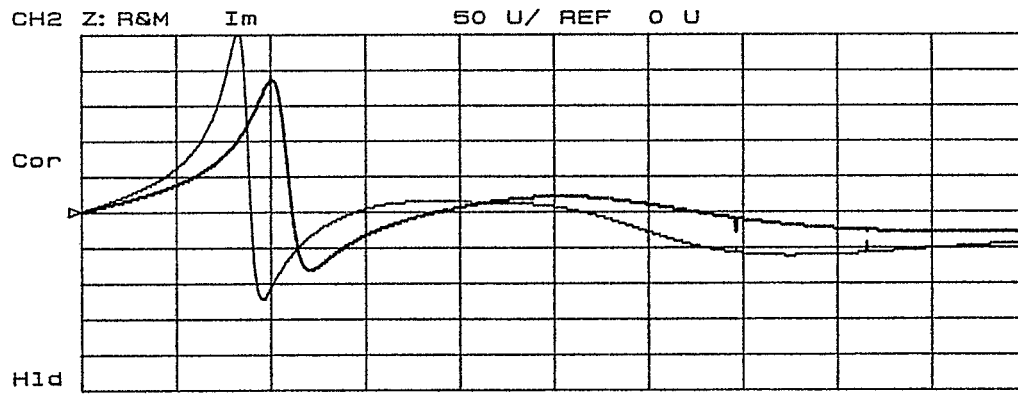
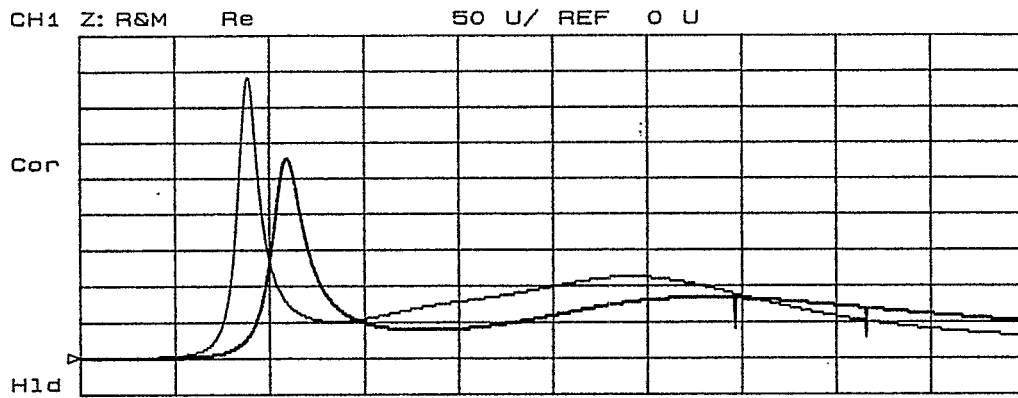


Fig. 8. Measured voltage of pulse at input and output end of the kicker. The measured transit time of ~50 nsec is confirmed by the P-Spice computations.

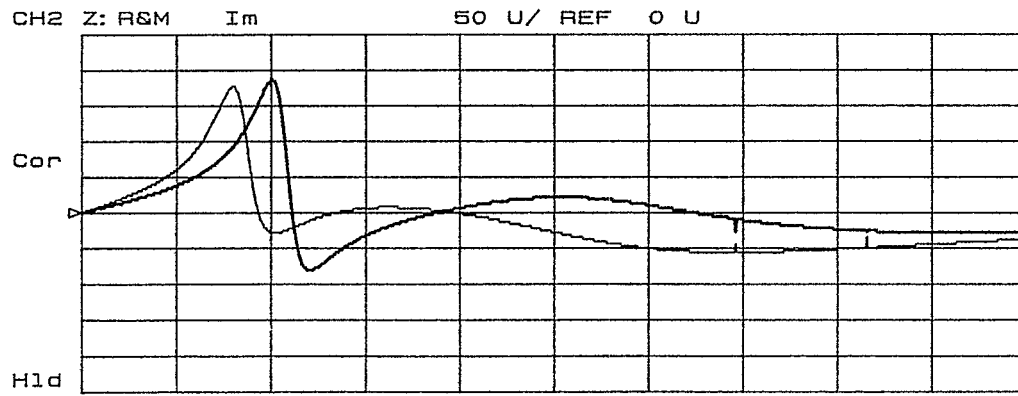
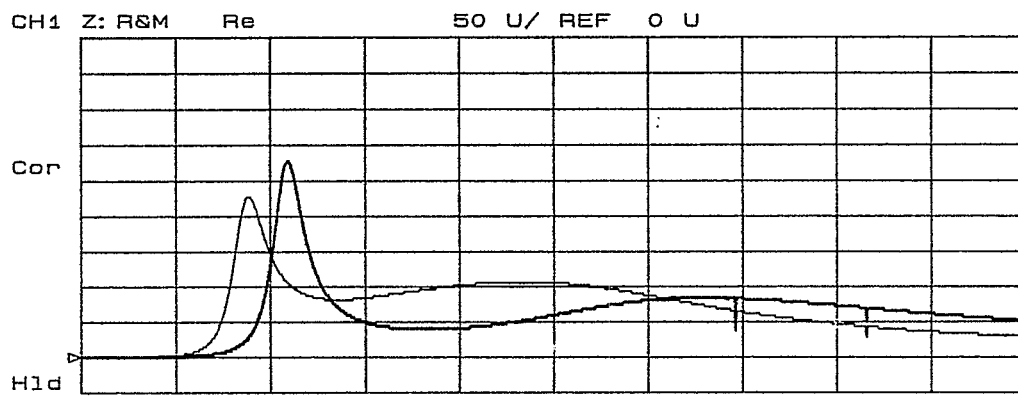
APPENDIX.

In an attempt to identify the origin of the "ferrite" resonance at ~ 64 MHz, a short, 12 inch long kicker model was assembled as erector set keeping the top fixed and varying the ferrite blocks in the sides. The top was formed from 4×1 in. dielectric blocks and 3×2 in. plus 2×1 in. ferrite blocks. The sides were to begin with formed in the standard $4 \times (2 + 1)$ in. arrangement. The input impedance of the shorted model was measured and stored in memory of the instrument as base for the subsequent changes. As seen in Fig. 9, the $\lambda/4$ - resonance at 4.76 MHz in the full size kicker has moved to ~ 21.2 MHz due to the reduced length of the model, but it is to be noted that the "ferrite" resonance remained almost unchanged at ~ 65 MHz.

The input impedance measured on the four models with changed length of the side ferrite blocks is shown in Fig. 9 for the case of 6×2 in. (top) plus 4×3 in. (bottom) and in Fig. 10 for the case of 6×2 in. (top) plus 1×12 in. (bottom). It is evident that the "ferrite" resonance depends strongly on the configuration of the side ferrites and that the use of "long" ferrite blocks, which would be more economical, is precluded by the increased losses and the lowered bandwidth.

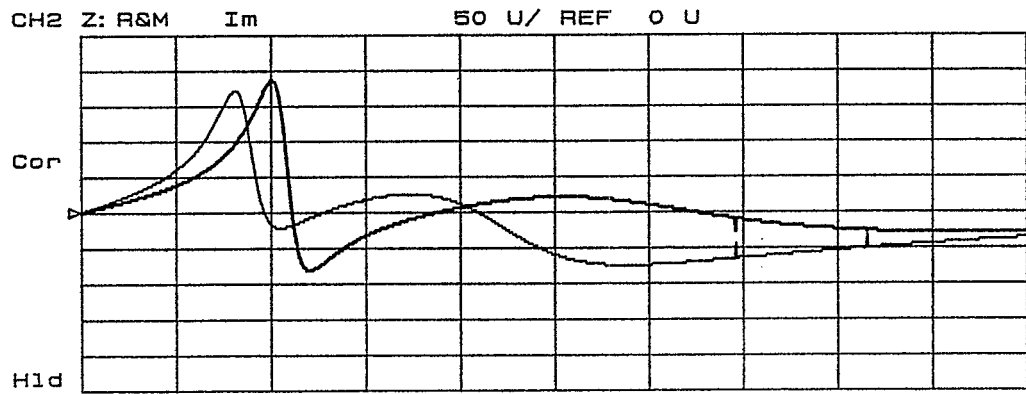
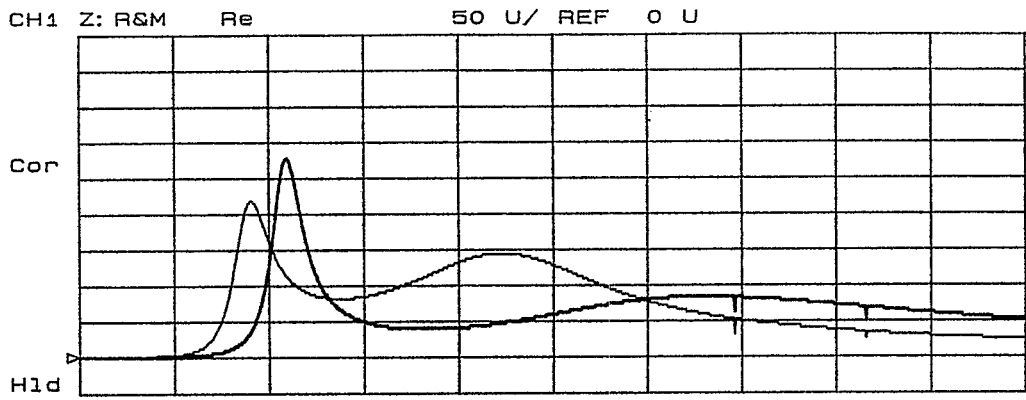


START 10 KHZ STOP 100 MHZ

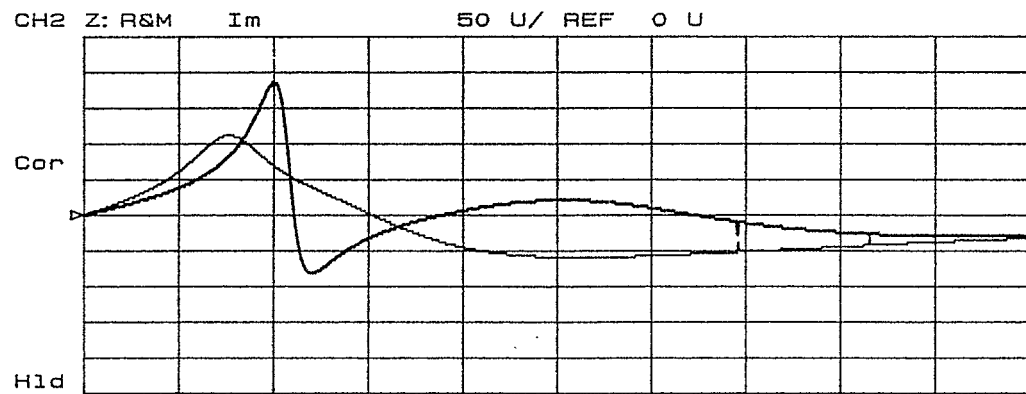
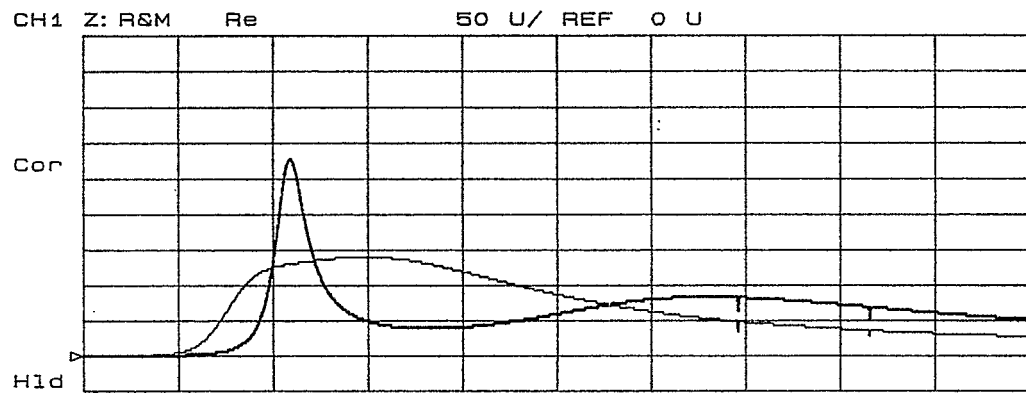


START 10 KHZ STOP 100 MHZ

Fig. 9. Measured input impedance of shorted 12 in. kicker model with ferrite side blocks, respectively 2 in. (top) and 3 in. (bottom) long. The darker curves represent a reference measurement with side blocks 2+1 in. long.

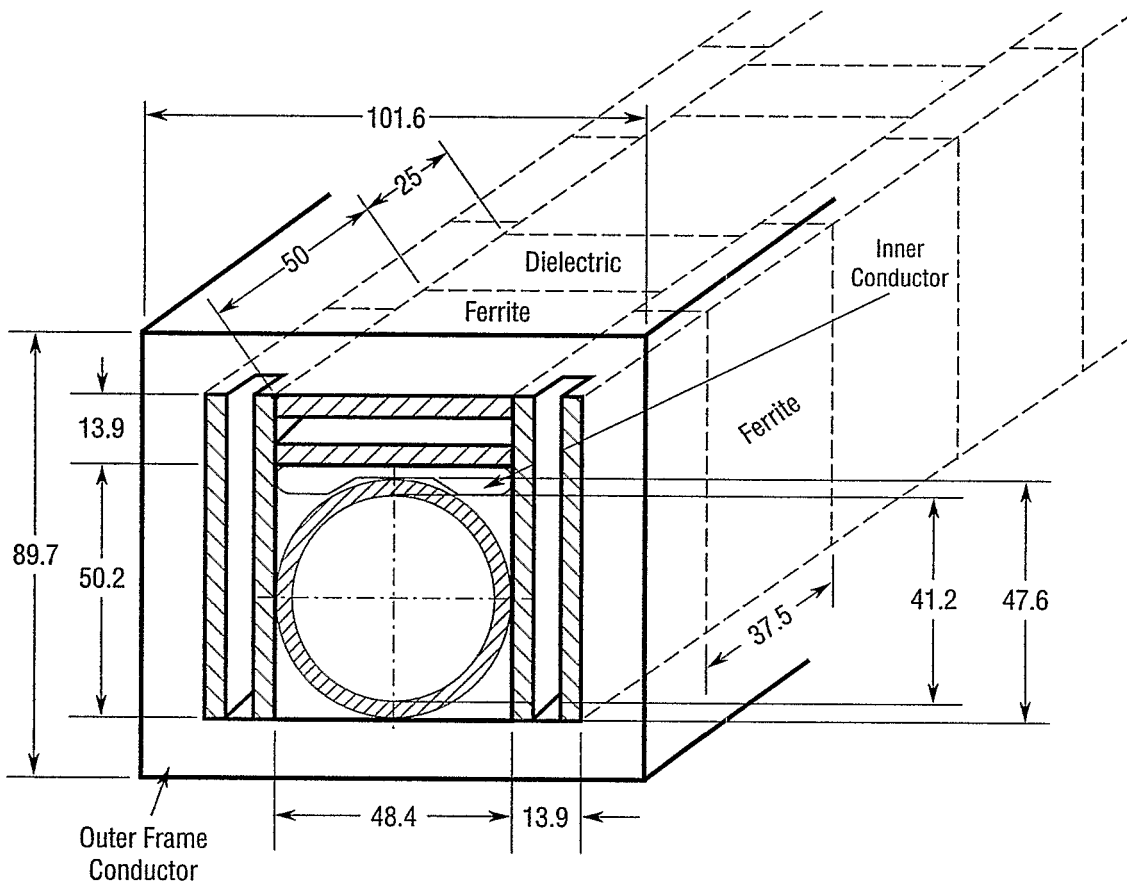


START 10 KHz STOP 100 MHz

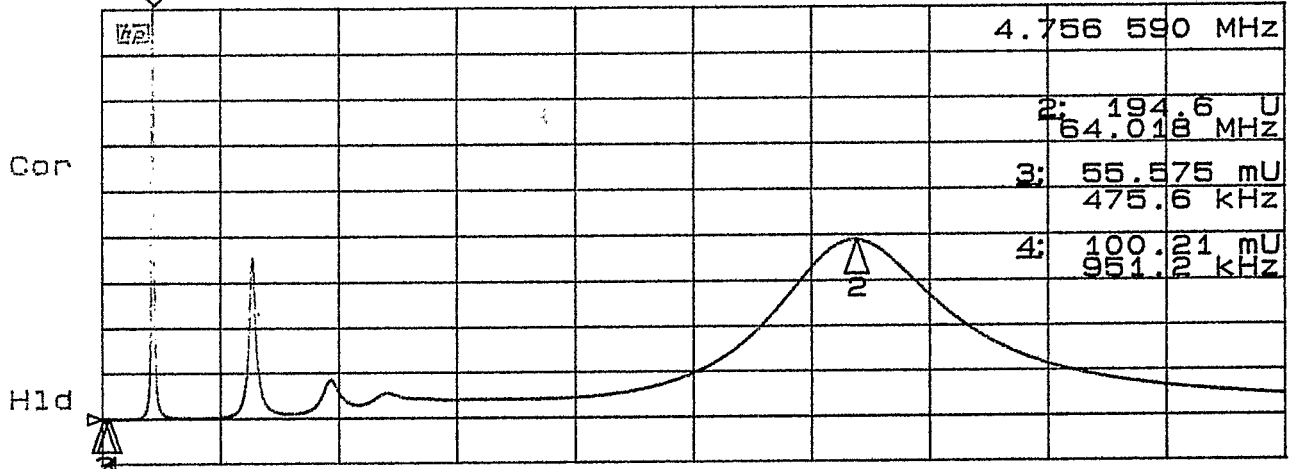


START 10 KHz STOP 100 MHz

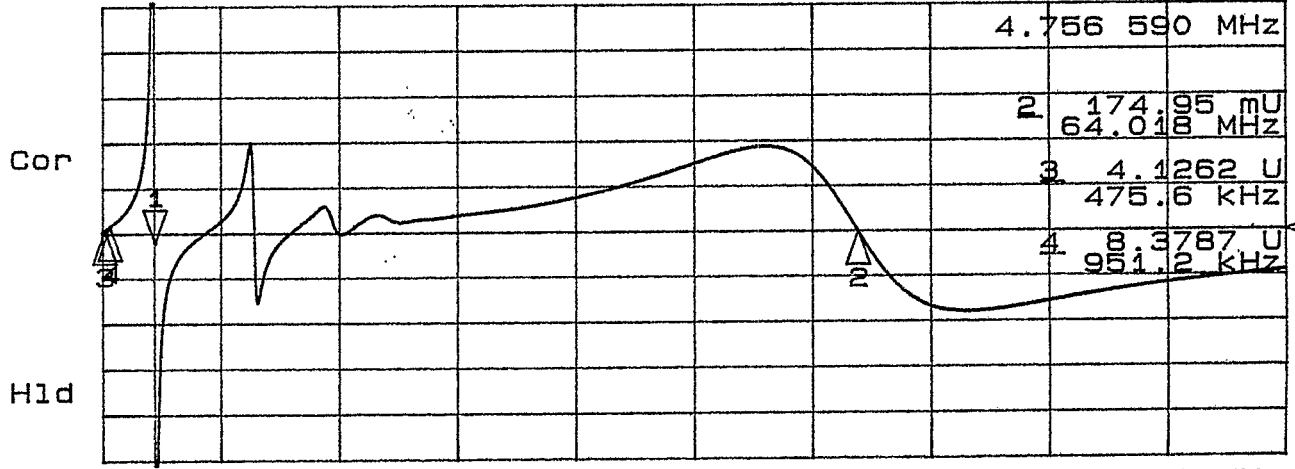
Fig. 10. Measured input impedance of a shorted 12 in. Kicker model with ferrite side blocks, respectively 6 in. (top) and 12 in. (bottom) long. The darker curves represent a reference measurement with side blocks 2+1 in. long.



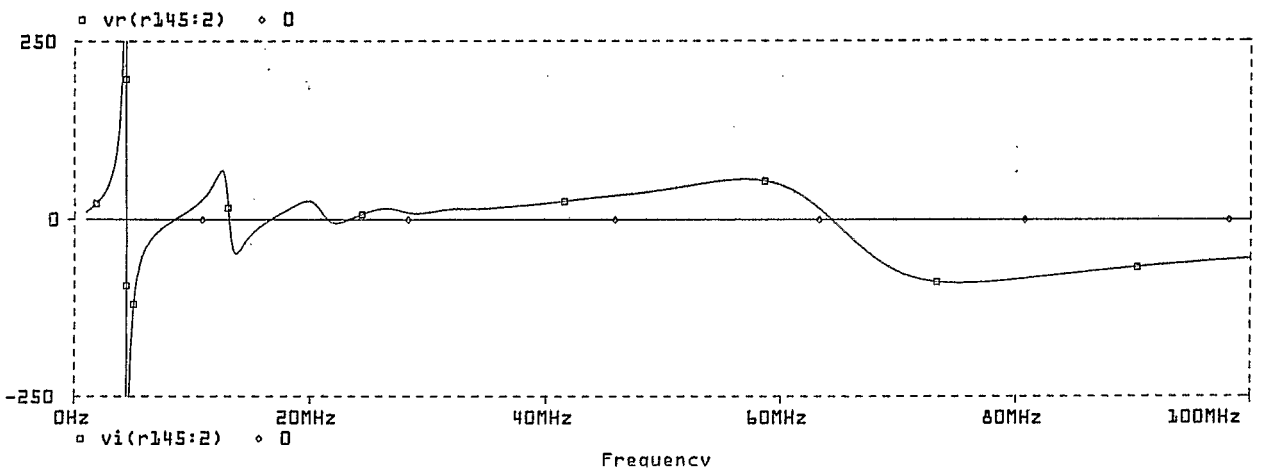
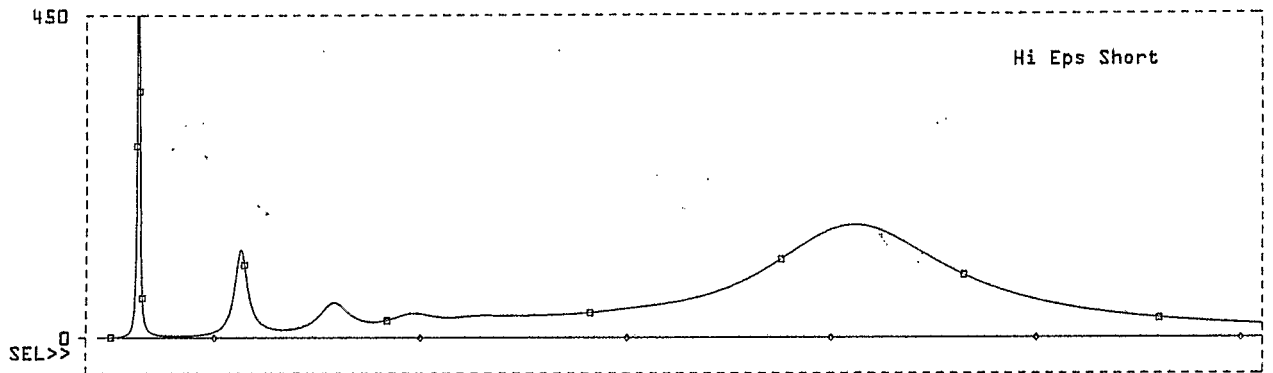
CH1 Z: μ Re 50 U/ REF 0 U 1: 1.076 KU



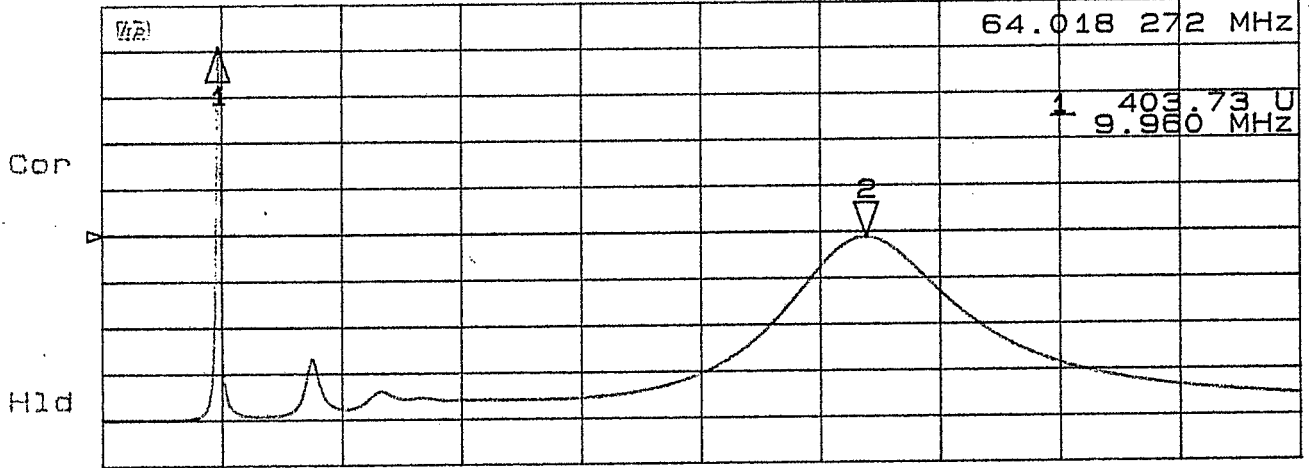
CH2 Z: R Im 50 U/ REF 0 U 1: -259.77 mU



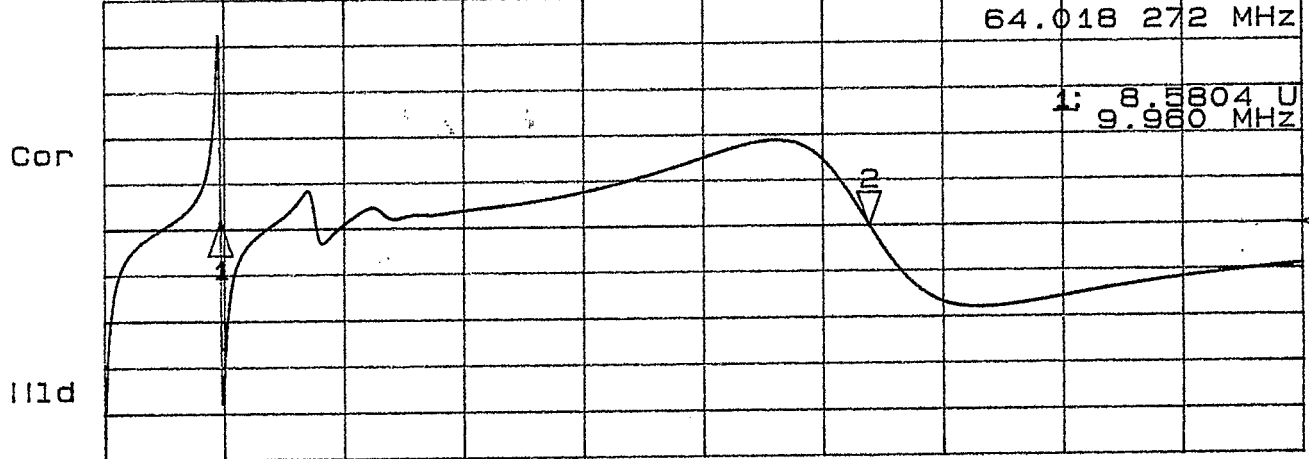
START .300 000 MHz STOP 100.000 000 MHz



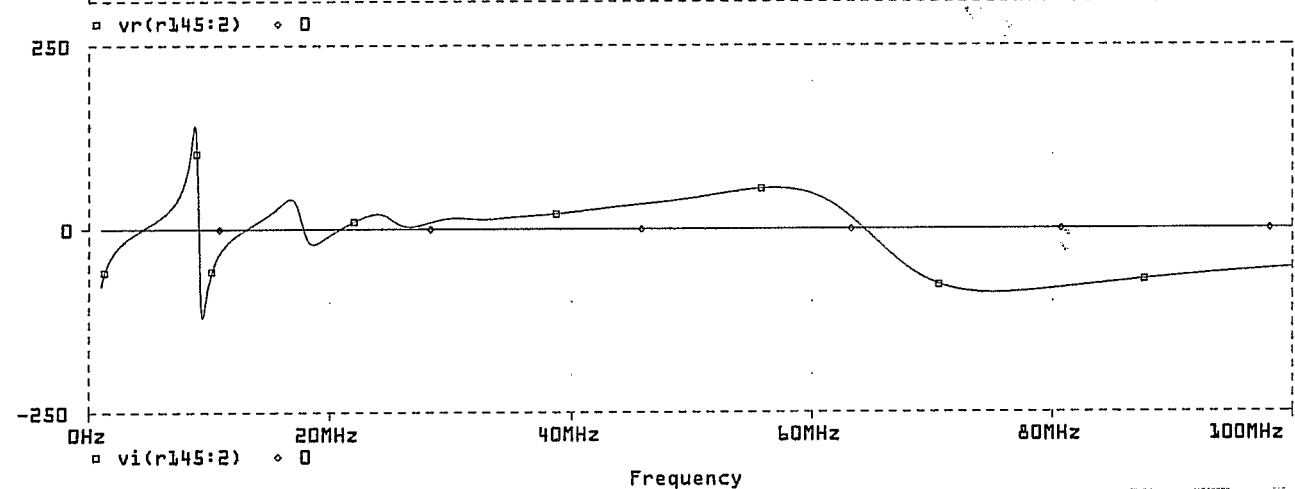
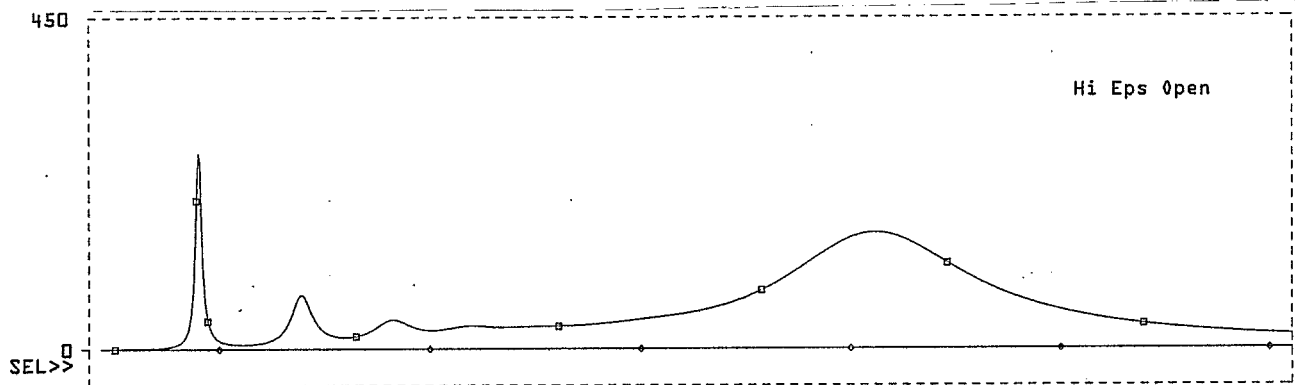
CH1 Z: R Re 50 U/ REF 200 U 2 194.36 U



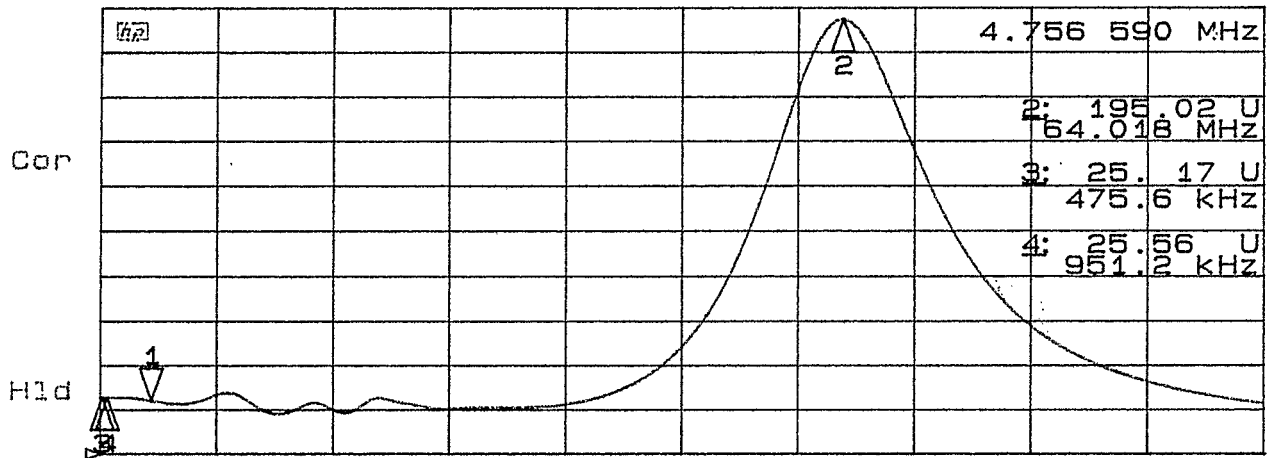
CH2 Z: R Im 50 U/ REF 0 U 2: -43.154 μ U



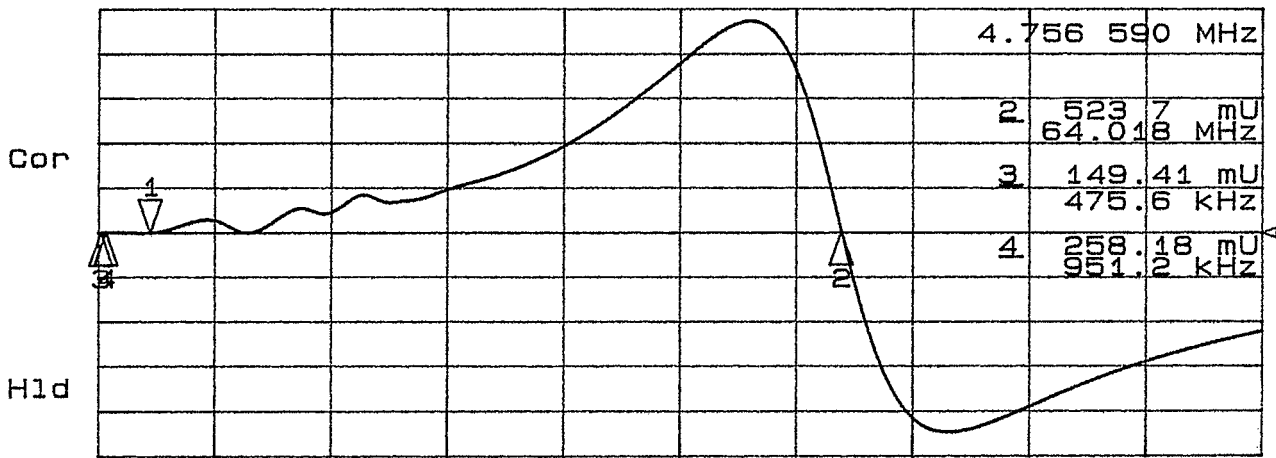
START .300 000 MHz STOP 100.000 000 MHz



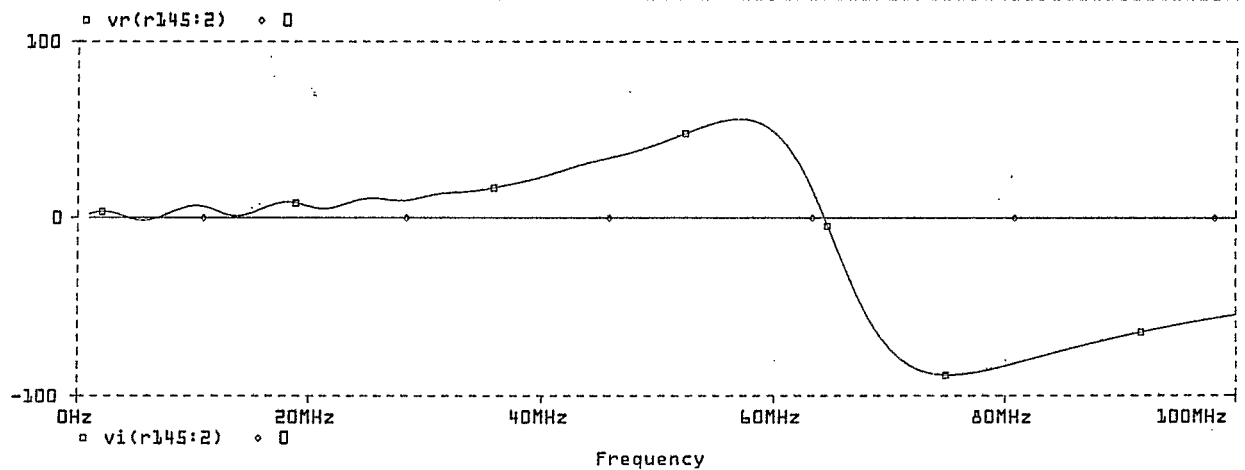
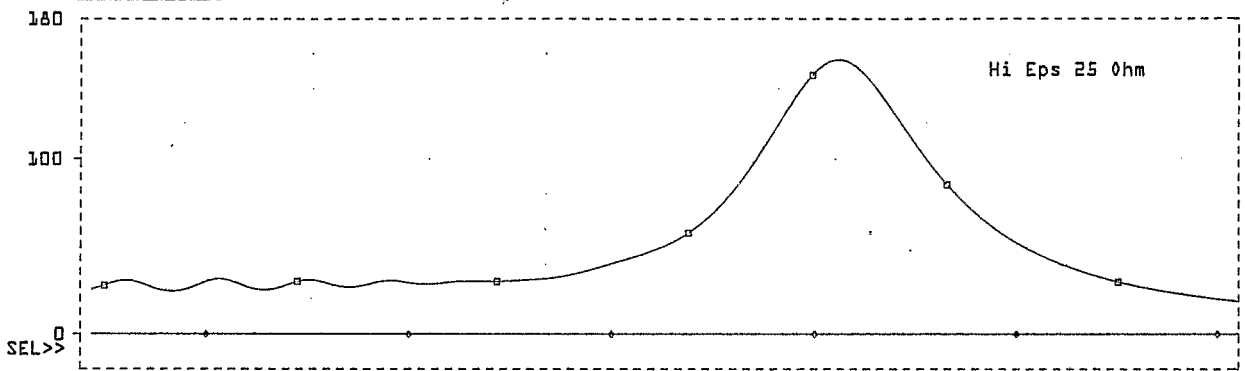
CH1 Z: R Re 20 U/ REF 0 U 1: 24.299 U

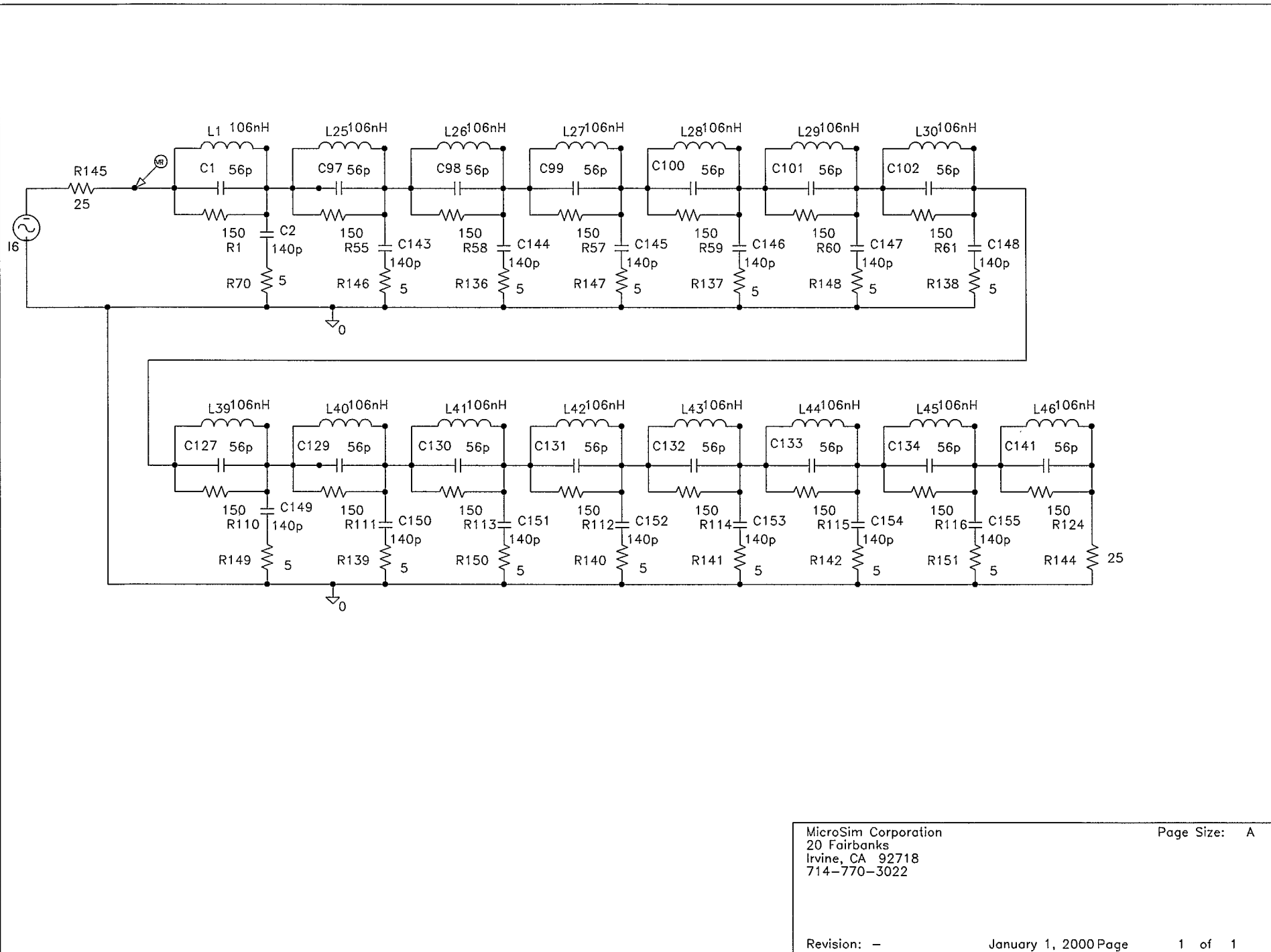


CH2 Z: R Im 20 U/ REF 0 U 1: 118.13 mU



START .300 000 MHz STOP 100.000 000 MHz





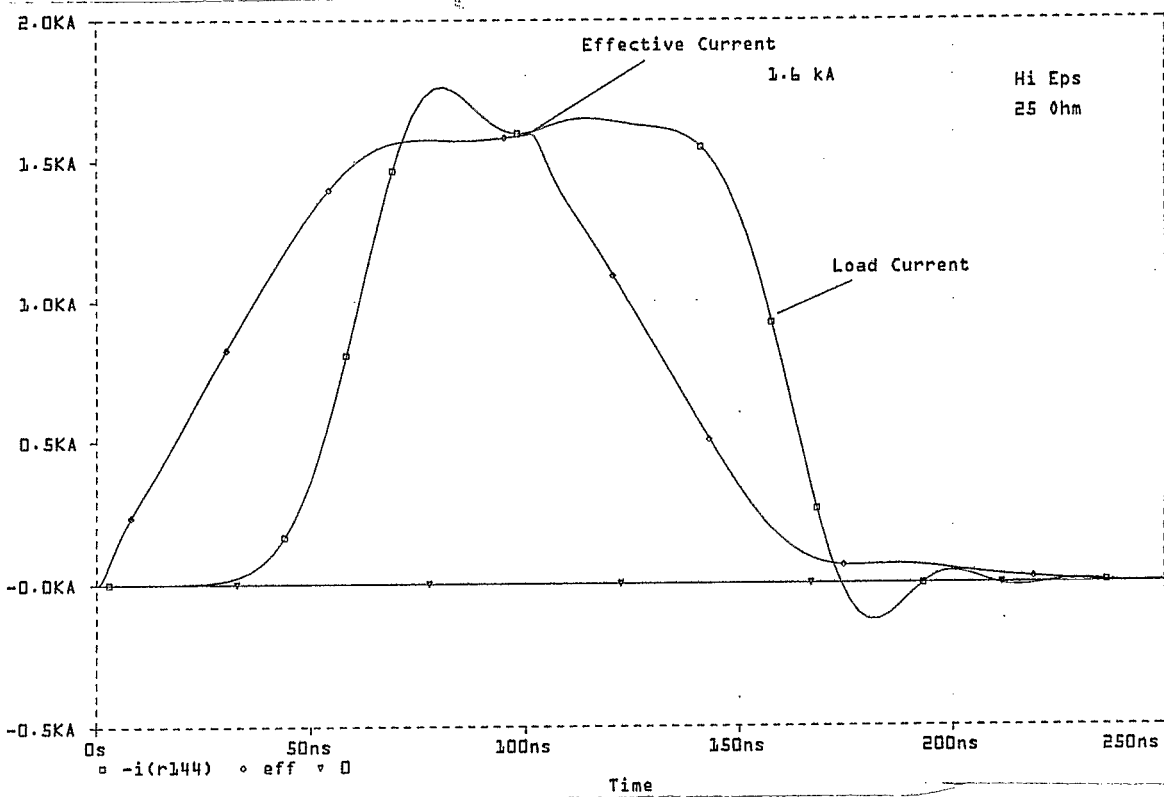
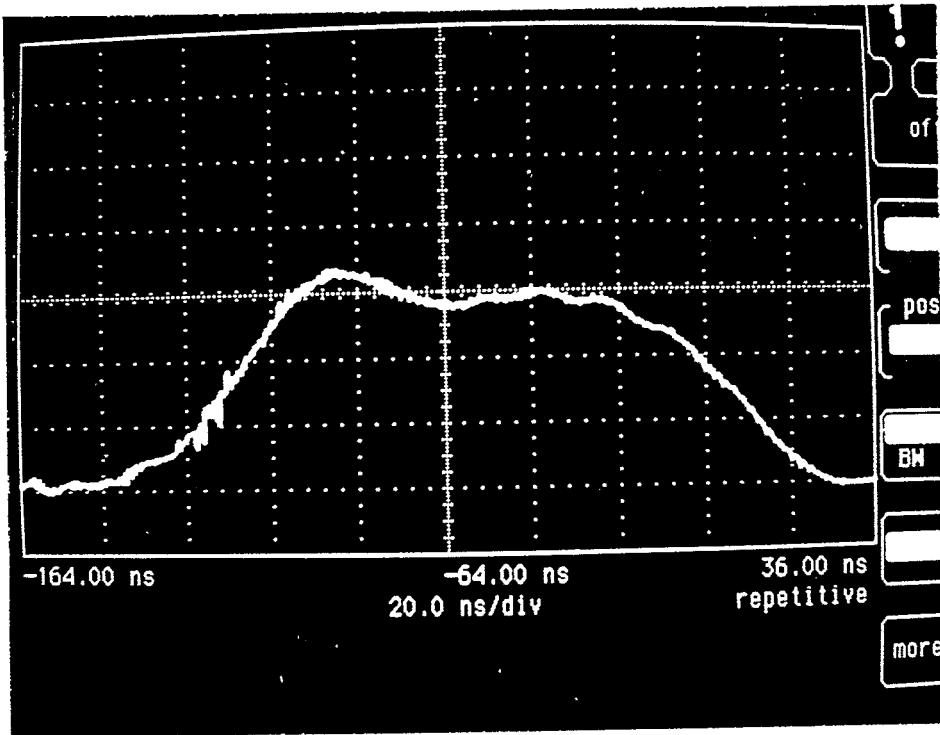
MicroSim Corporation
 20 Fairbanks
 Irvine, CA 92718
 714-770-3022

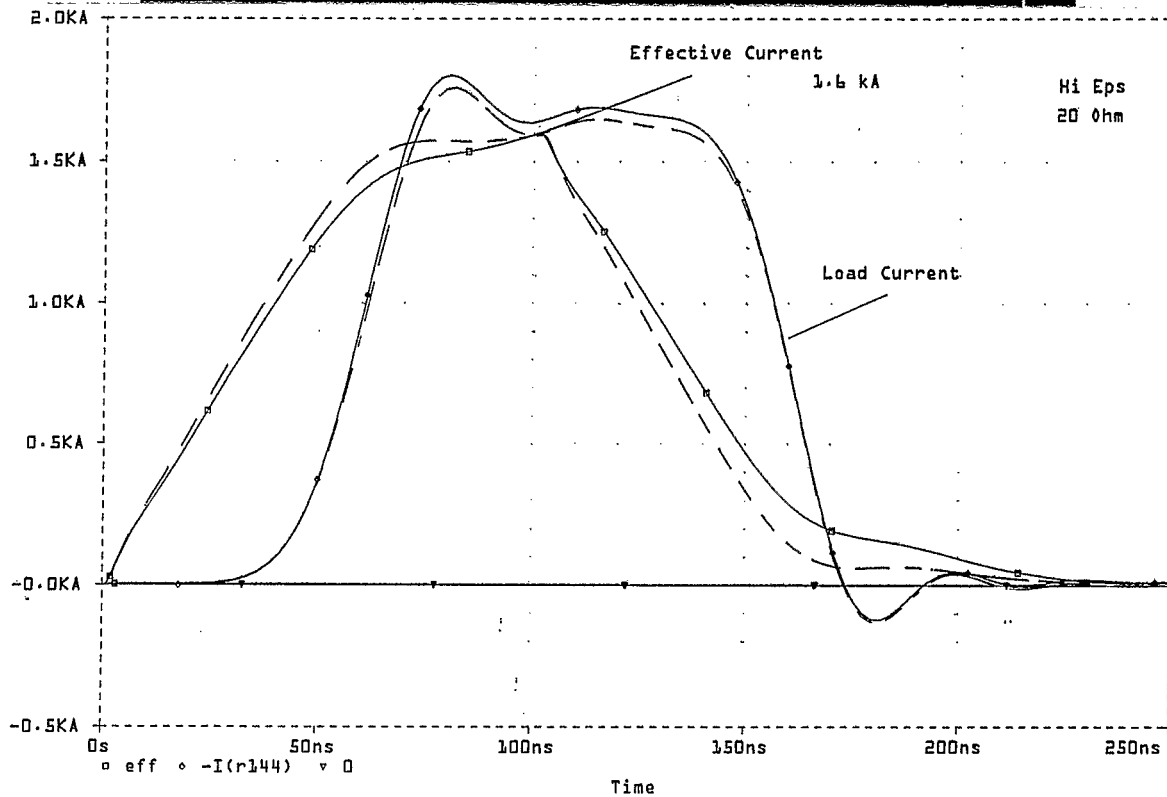
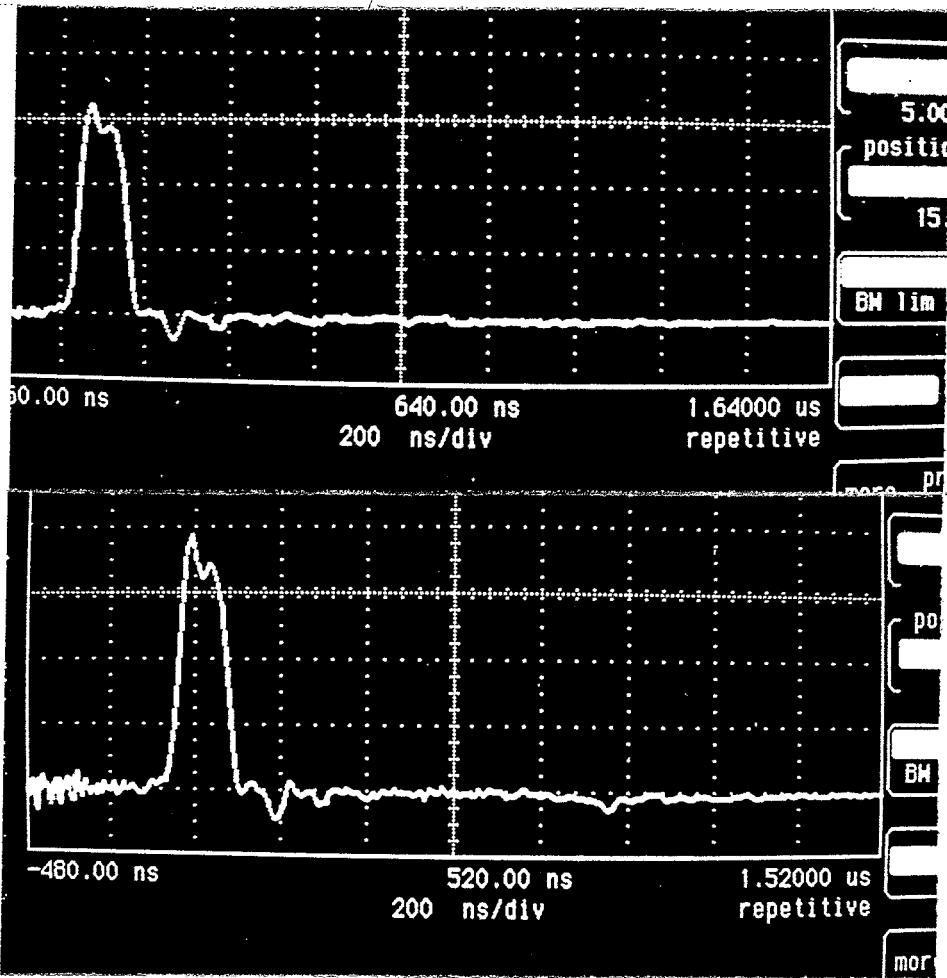
Page Size: A

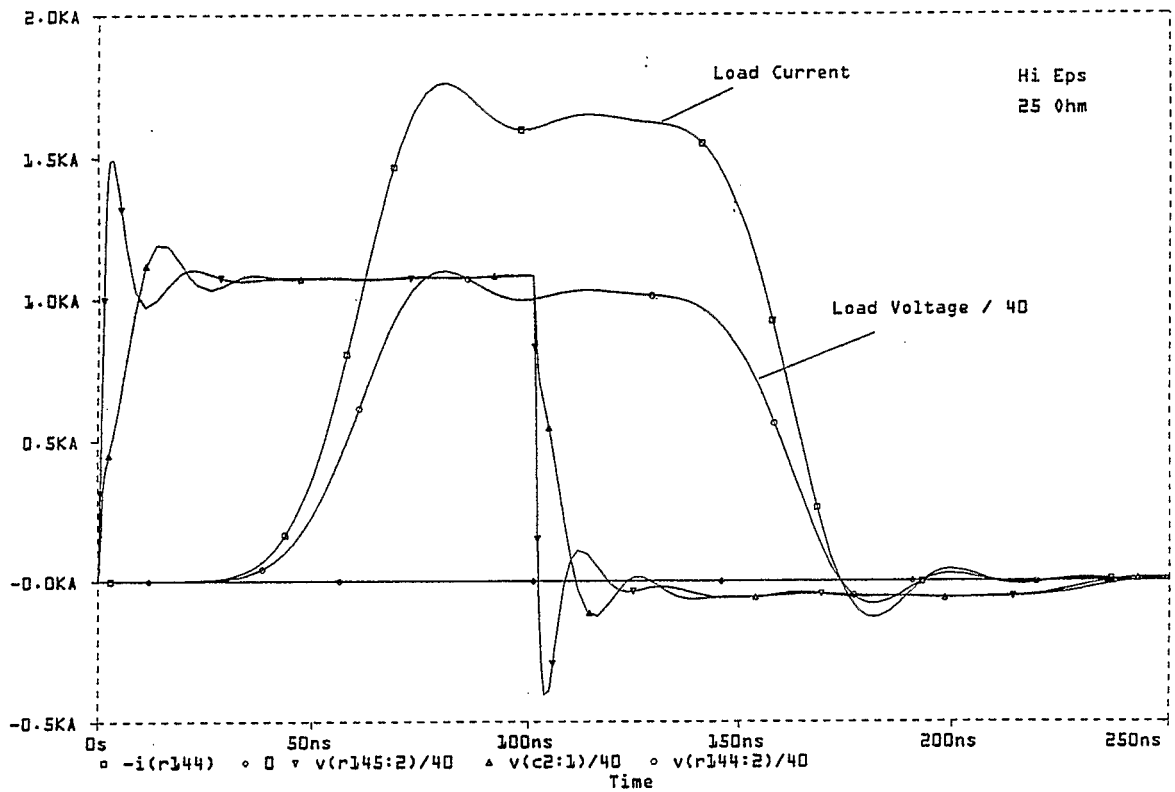
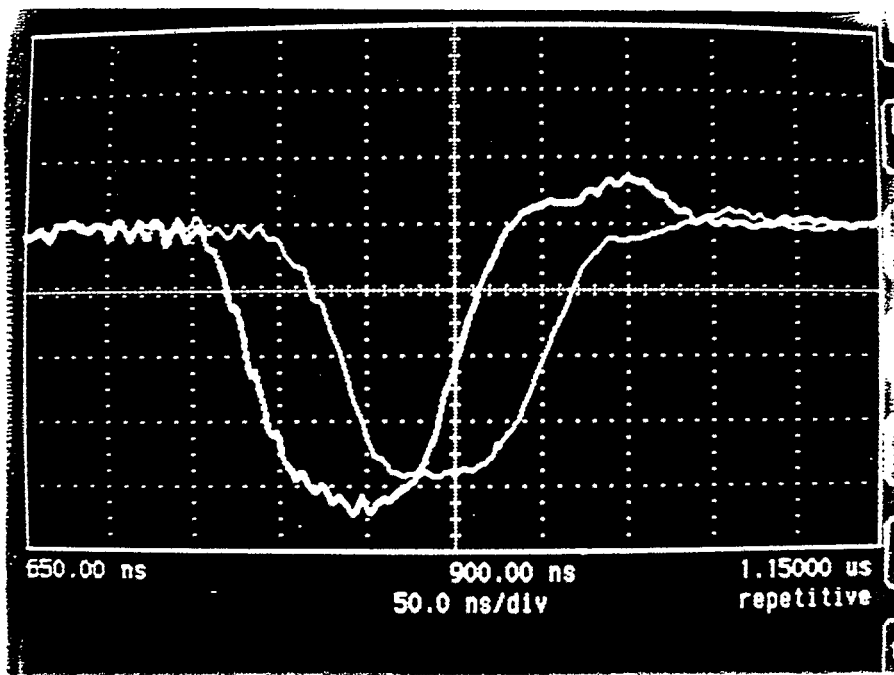
Revision: -

January 1, 2000 Page

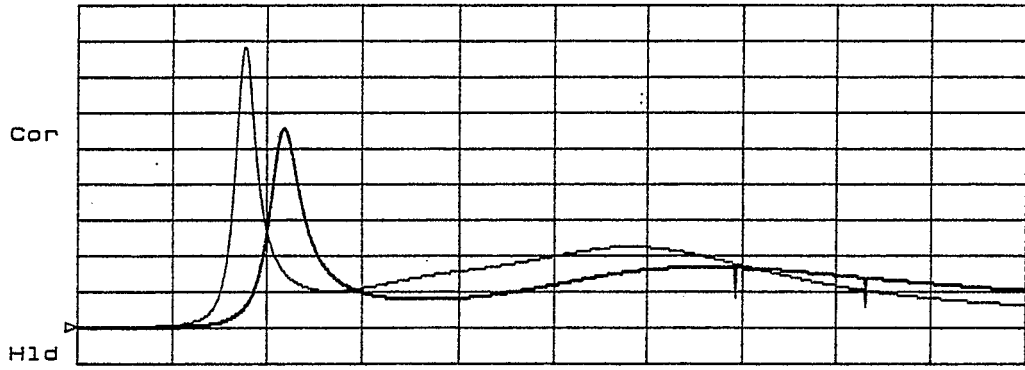
1 of 1



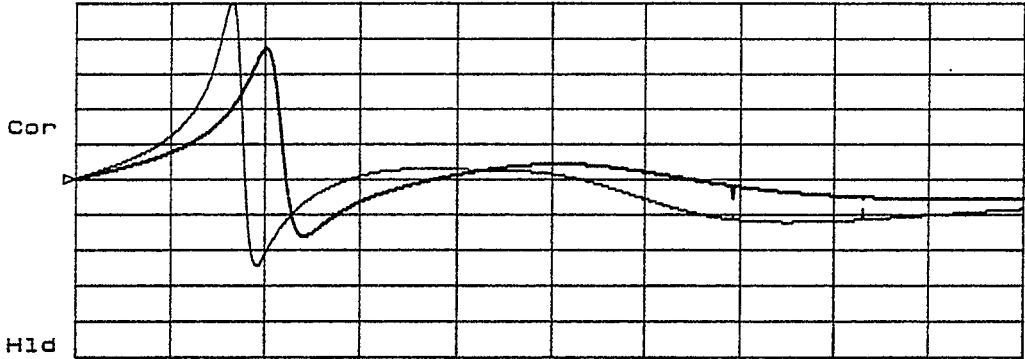




CH1 Z: R&M Re 50 U/ REF 0 U



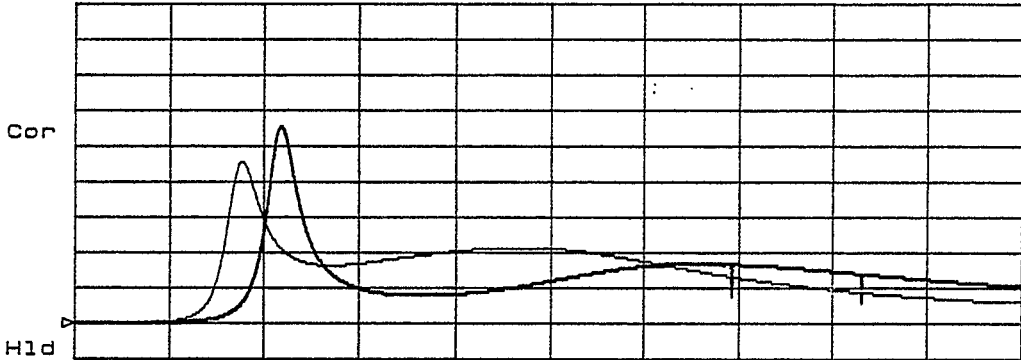
CH2 Z: R&M Im 50 U/ REF 0 U



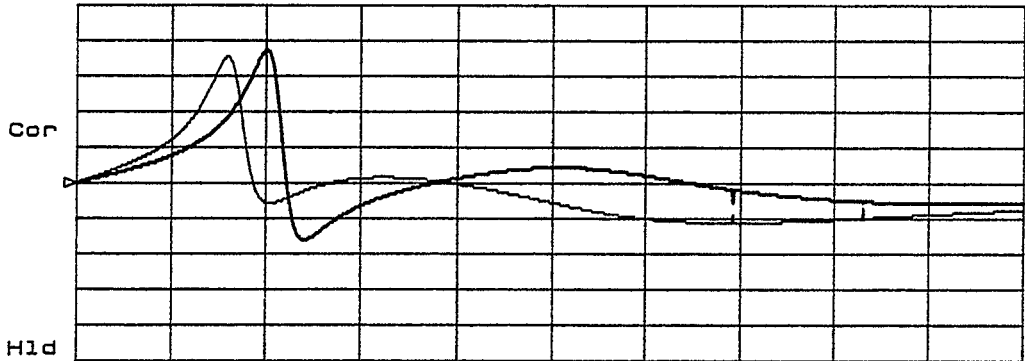
START 10 KHz

STOP 100 MHz

CH1 Z: R&M Re 50 U/ REF 0 U



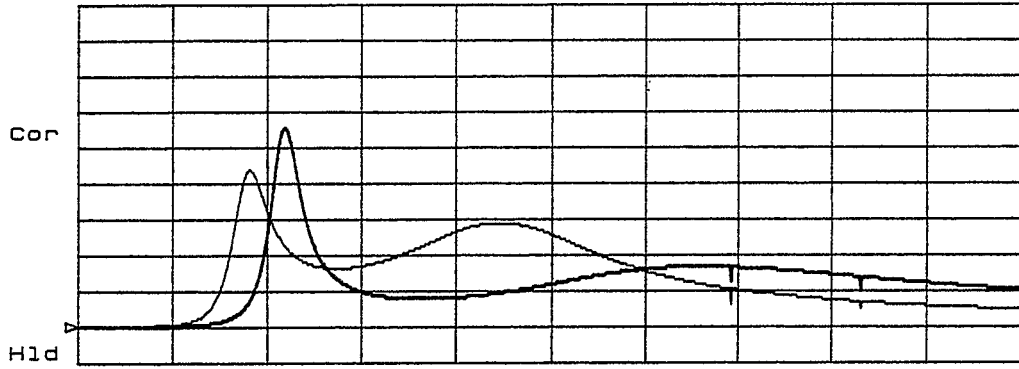
CH2 Z: R&M Im 50 U/ REF 0 U



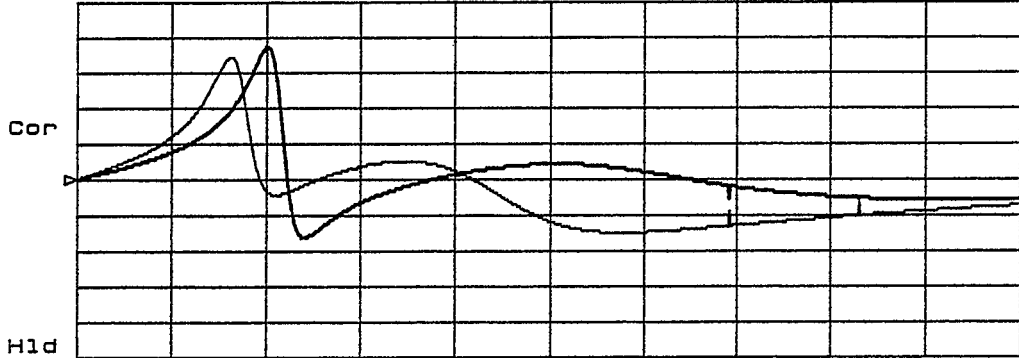
START 10 KHz

STOP 100 MHz

CH1 Z: R&M Re 50 U/ REF 0 U



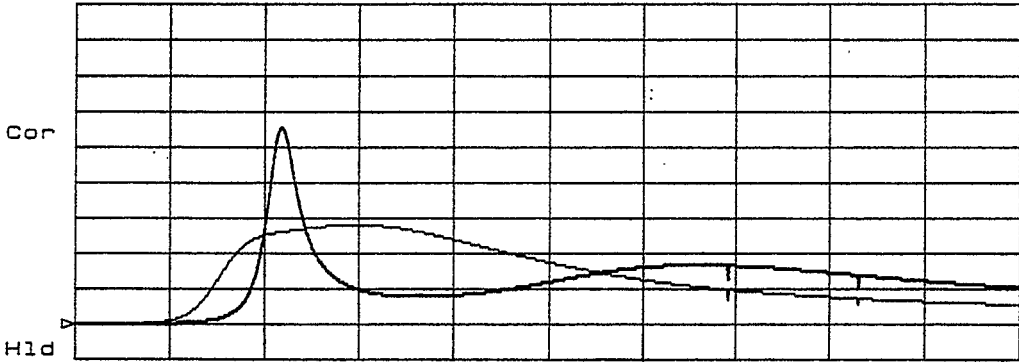
CH2 Z: R&M Im 50 U/ REF 0 U



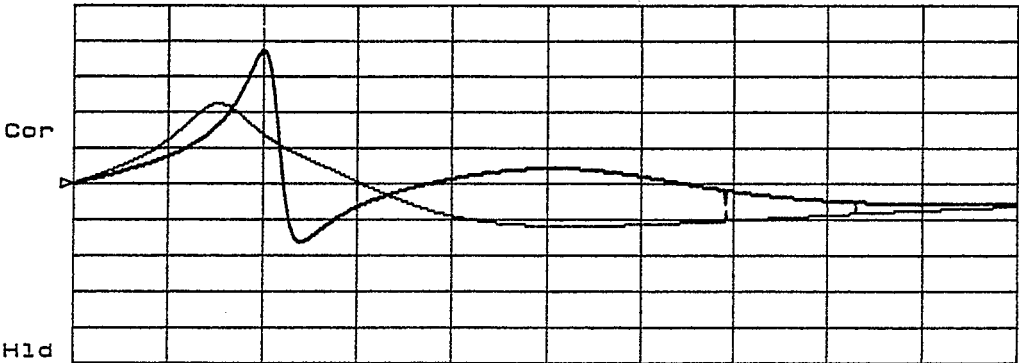
START 10 KHz

STOP 100 MHz

CH1 Z: R&M Re 50 U/ REF 0 U



CH2 Z: R&M Im 50 U/ REF 0 U



START 10 KHz

STOP 100 MHz